

# **Research Achievements of SC Structure and Strength Evaluation of US-APWR SC Structure Based on 1/10<sup>th</sup> Scale Test Results**

**Non-proprietary Version**

**December 2012**

**©2012 Mitsubishi Heavy Industries, Ltd.  
All Rights Reserved**

## **Revision History**

Revision	Page	Description
0	All	Original Issue
1	Sections 1, 2.3, 4, and 5, Appendix A, B, C, D, and E Editorial changes made throughout	Revision to add a summary of the SC module test research papers and the test results applicability to the US-APWR CIS. This incorporates responses to RAI 858-6126 Question 03.08.03-45, 894-6270 Question 03.08.03-66, and 958-6608 Question 03.08.03-93. This included addition of Appendix A through D with supporting discussion in the Abstract and sections 1.0, 2.3, and 4. Research reference papers listed in section 5 and copies provided in Appendix E. Various editorial changes and corrections made.

© 2012

**MITSUBISHI HEAVY INDUSTRIES, LTD.**

All Rights Reserved

This document has been prepared by Mitsubishi Heavy Industries, Ltd. ("MHI") in connection with the U.S. Nuclear Regulatory Commission's ("NRC") licensing review of MHI's US-APWR nuclear power plant design. No right to disclose, use or copy any of the information in this document, other than by the NRC and its contractors in support of the licensing review of the US-APWR, is authorized without the express written permission of MHI.

This document contains technology information and intellectual property relating to the US-APWR and it is delivered to the NRC on the express condition that it not be disclosed, copied or reproduced in whole or in part, or used for the benefit of anyone other than MHI without the express written permission of MHI, except as set forth in the previous paragraph.

This document is protected by the laws of Japan, U.S. copyright law, international treaties and conventions, and the applicable laws of any country where it is being used.

Mitsubishi Heavy Industries, Ltd.  
16-5, Konan 2-chome, Minato-ku  
Tokyo 108-8215 Japan

## **Abstract**

The purpose of this Technical Report (TeR) is to present the research achievements for steel-concrete (SC) structure and the strength evaluation of SC structure of the US-APWR standard plant.

This TeR describes:

- Research achievements for SC structure
- The evaluation of US-APWR SC structure includes;  
Comparison of the typical dimensions  
Comparison of sectional property  
Comparison of ultimate strength of SC module  
Safety margin against the design forces applied on SC modules which comprise the US-APWR Containment Internal Structure (CIS)
- The conclusion of the research evaluation in confirming the conservatism of the US-APWR SC structures.

Revision 1 of this report includes the addition of Appendix A, B, C, and D. These appendices provide a summary of the SC experimental database and the test results applicability to the US-APWR CIS. The full research reports are provided in Appendix E.

This technical report presents only existing research available on SC structures. Confirmatory physical testing performed specifically for the US-APWR design is presented in TeR MUAP-11013.

## Table of Contents

List of Acronyms	ii
List of Figures	iii
List of Tables	iv
1.0 INTRODUCTION	1
2.0 RESEARCH ACHIEVEMENTS FOR SC STRUCTURE	2
2.1 Outline of SC Structure and Research History	2
2.2 Overview of Research Achievements for SC Structure	4
2.3 Overview of Experimental Database for SC Structure	14
3.0 STRENGTH EVALUATION OF US-APWR SC MODULES	15
3.1 Methodology of the Evaluations	15
3.2 Evaluation Results	16
3.2.1 Comparison of Typical Dimensions	16
3.2.2 Comparison of Sectional Properties	22
3.2.3 Comparison of Ultimate Strength of SC Wall Members	25
3.2.4 Safety Margin Against the Design Applied Forces of US-APWR CIS	27
4.0 CONCLUSION	32
4.1 Research Achievements	32
4.2 Experimental Database	32
5.0 REFERENCES	33
APPENDIX A EXPERIMENTAL DATABASE AND US-APWR SC WALL DESIGN	
APPENDIX B OUT-OF-PLANE EXPERIMENTAL DATABASE AND COMPARISON WITH DESIGN EQUATION	
APPENDIX C IN PLANE SHEAR DATABASE AND COMPARISON WITH DESIGN EQUATION	
APPENDIX D AXIAL COMPRESSION AND LOCAL BUCKLING DATABASE AND COMPARISON WITH DESIGN EQUATION	
APPENDIX E RESEARCH REFERENCES	

## List of Acronyms

CIS	Containment Internal Structure
DCD	Design Control Documents
FEM	Finite Element Model
LOCA	Loss of Coolant Accident
NPP	Nuclear Power Plants
NRC	Nuclear Regulatory Commission
PWR	Pressurized Water Reactor
RC	Reinforced Concrete
SC	Steel Concrete
SRRC	Steel Reinforcement Ratio Category
SSC	Structures, Systems, and Components
TeR	Technical Report
US	United States

## List of Figures

Figure 2-1	Outline of SC Module	2
Figure 2-2	Load Relative Rotation Angle Relationship	4
Figure 2-3	Specimen (BS70T10)	5
Figure 2-4	Relationship of Load and Deformation (BS70T10)	5
Figure 2-5	Finite Element Model	6
Figure 2-6	Relation of Load and Rotation Angle	6
Figure 2-7	Experimental Equipment and Displacement Measuring Point	7
Figure 2-8	Result of Axial Deformation	7
Figure 2-9	Relation of Shear Force and Shear Strain	8
Figure 2-10	Crack Propagation (CA)	9
Figure 2-11	Relation of b/t and Buckling Strain	9
Figure 2-12	Loading Method	10
Figure 2-13	Relation of Load and Displacement	10
Figure 2-14	A Sample of SC Design Recommendation	11
Figure 2-15	Loading System of Pure Shear Force	12
Figure 2-16	Specimens of SC, Half SC and RC	13
Figure 2-17	Cracking of SC, Half SC and RC	13
Figure 3-1	Comparison of Dimensions	17
Figure 3-2	Plan of SC Modules for US-APWR CIS	18
Figure 3-3	Section of SC Modules for US-APWR CIS	19
Figure 3-4	SC Module Plan of 1/10 <sup>th</sup> Scale Model	20
Figure 3-5	SC Module Section of 1/10 <sup>th</sup> Scale Model	21
Figure 3-6	Comparison of Sectional Properties	23
Figure 3-7	Overview Plan of US-APWR	24

### List of Figures (continued)

Figure 3-8	Overview Plan of 1/10 <sup>th</sup> Scale Model	24
Figure 3-9	Overview of SC Modules Wall Member	26
Figure 3-10	Comparison of SC Wall Member Strengths	26
Figure 3-11	Load-Displacement Curve of 1/10 <sup>th</sup> Scale Model	28
Figure 3-12	Distribution of Design Shear Force and Bending Moment for the US-APWR	29
Figure 3-13	Margin for Design Forces of the US-APWR	30

### List of Tables

Table 2-1	Research History of SC Structure	3
Table 3-1	Comparison of Dimensions	17
Table 3-2	Comparison of Sectional Properties	23
Table 3-3	Material Properties of SC Modules	25
Table 3-4	Comparison of SC Wall Member Strengths	26
Table 3-5	Margin for Design Force of the US-APWR (1)	30
Table 3-6	Estimated Ultimate Capacity of SC Modules in the US-APWR CIS	31
Table 3-7	Margin for Design Force of the US-APWR (2)	31

## 1.0 INTRODUCTION

Currently, design codes for Steel-Concrete (SC) structures are available in Japan as “Technical Code for Aseismic Design of Steel Plate Reinforced Concrete Structures (JEAC 4618-2009)”. Similar codes or guidelines specifically applied to SC structures are not currently available in the United States (US). However, it is known that US design codes or guidelines are under preparation, and will be codified by US standards in the future.

A SC structure is typically constructed of multiple SC Modules. In the case of the US-APWR, the containment internal structure (CIS) is designed as a SC structure utilizing several SC modules. In SC structure research, the CIS was also referred to as the inner concrete structure. Since there are no specific US design codes applicable to SC modules, the SC modules are conservatively designed utilizing criteria based on ACI-349-06 requirements for conventional reinforced concrete structures.

The amended response (MHI Letter UAP-HF-09449 dated September 17, 2009) to RAI 322-1999 regarding the SC modules in the CIS discussed in Design Control Document (DCD) Subsection 3.8.3 also addresses the soundness of SC modules under accident and fire events.

Revision 0 of this Technical Report (TeR) introduced 10 research achievements of SC structures. In addition, this TeR confirms that the SC modules have sufficient capacity and safety allowance to applied loads when designed using criteria based on ACI-349-06, based on the experimental results obtained by the static load tests of a 1/10<sup>th</sup> scale model of SC structures conducted by MHI in the past.

Revision 1 of this TeR adds additional references and an overview of the experimental database for SC composite structures that applies to the US-APWR. Appendix A through D provides a summary of the experimental database found in 12 research references and compares it with the US-APWR design equations to confirm that design strengths for SC walls can be conservatively estimated using US-APWR design equations. The term SC walls is used to refer to a portion of an SC module within these appendices. Appendix E provides copies of 19 research papers referred to in US-APWR TeRs.

This TeR presents only existing research available on SC structures. Confirmatory physical testing performed specifically for the US-APWR design is presented in TeR MUAP-11013.

## **2.0 RESEARCH ACHIEVEMENTS FOR SC STRUCTURE**

### **2.1 Outline of SC Structure and Research History**

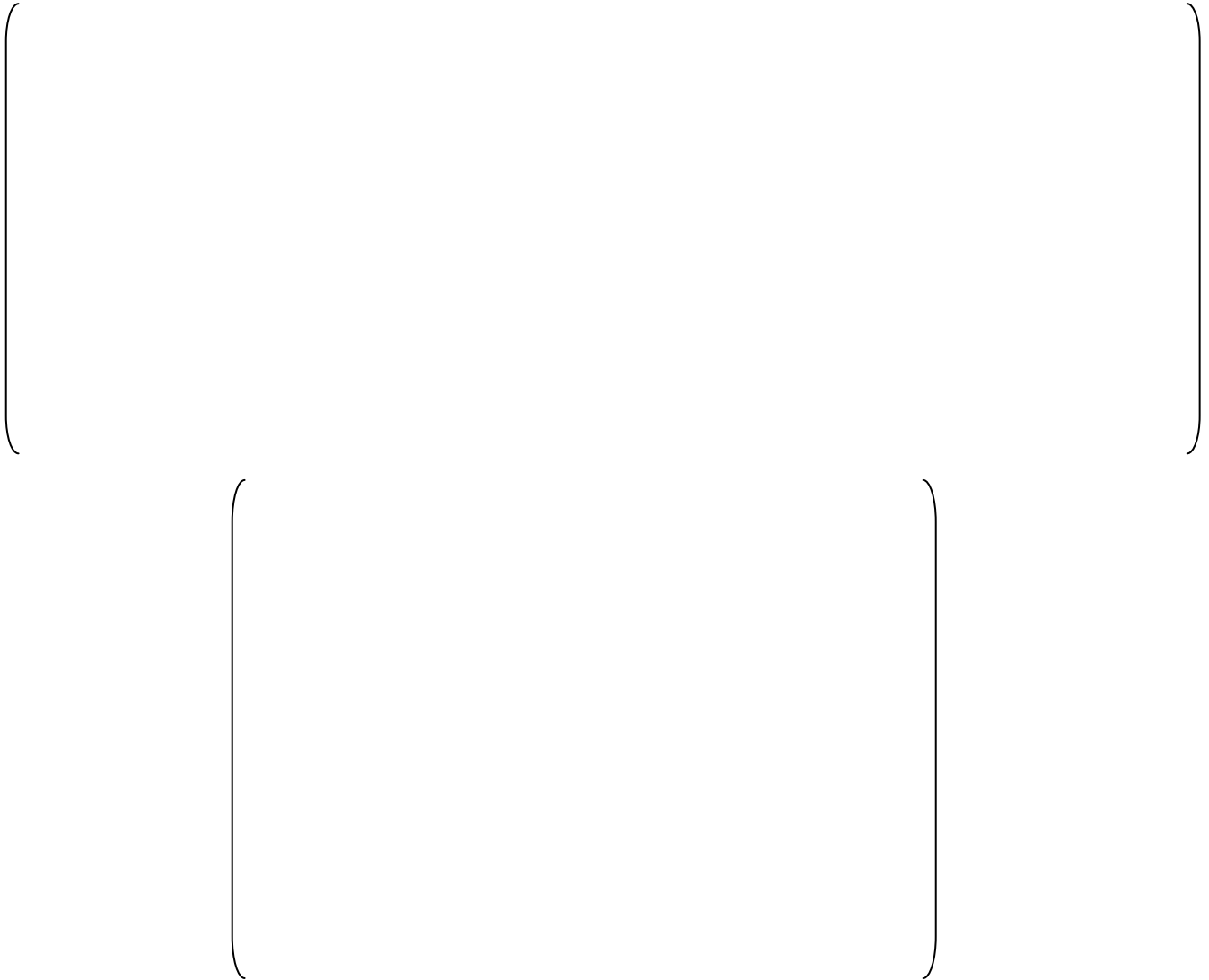


**Figure 2-1 Outline of SC Module**



**Table 2-1 Research History of SC Structure**



## 2.2 Overview of Research Achievements for SC Structure

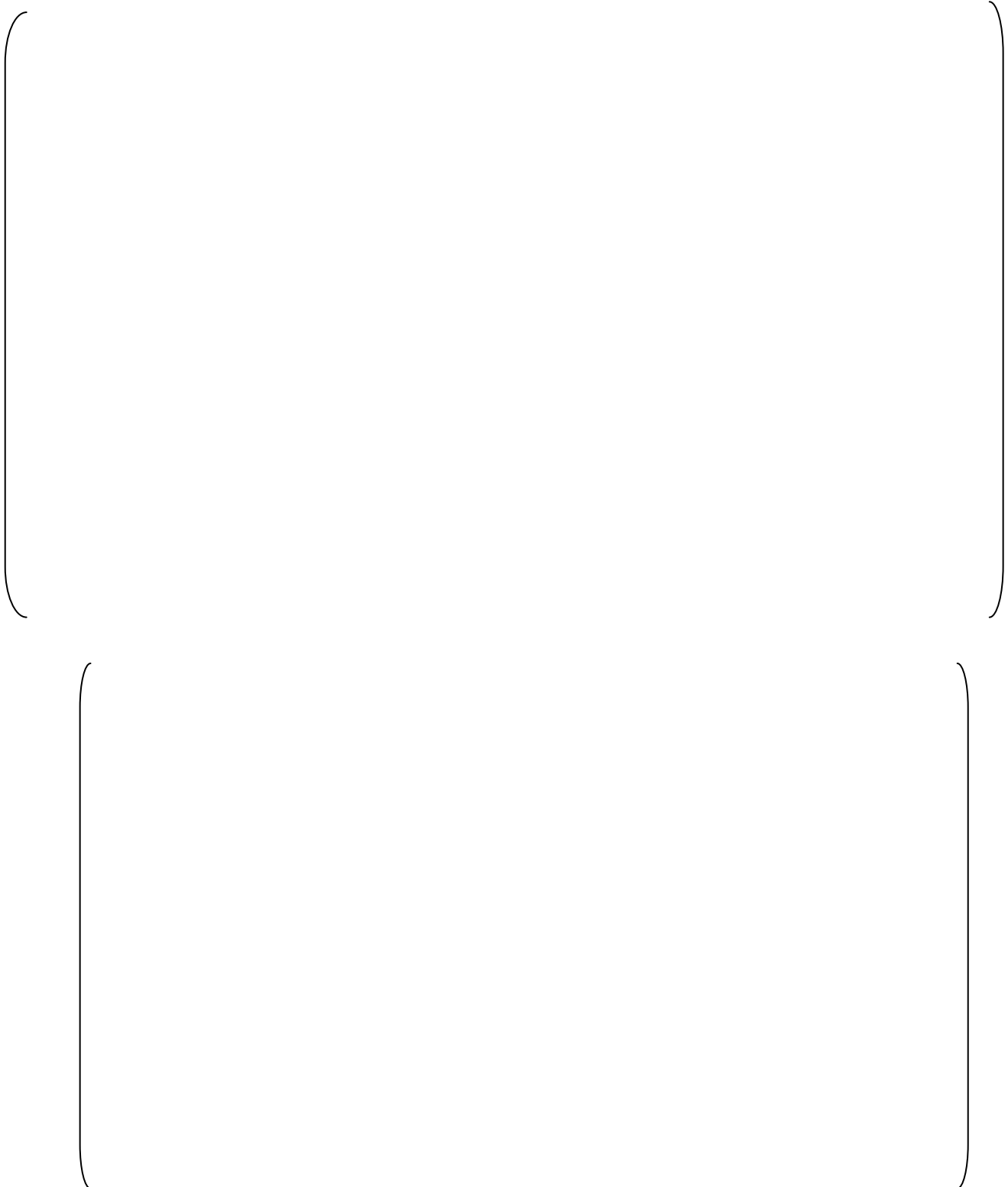


**Figure 2-2 Load Relative Rotation Angle Relationship**



**Figure 2-3 Specimen (BS70T10)**



**Figure 2-4 Relation of Load and Deformation  
(BS70T10)**



**Figure 2-5 Finite Element Model**



**Figure 2-6 Relationship of Load and Rotation angle**



**Figure 2-7 Experimental  
Equipment and Displacement  
Measuring Point**



**Figure 2-8 Result of Axial Deformation**

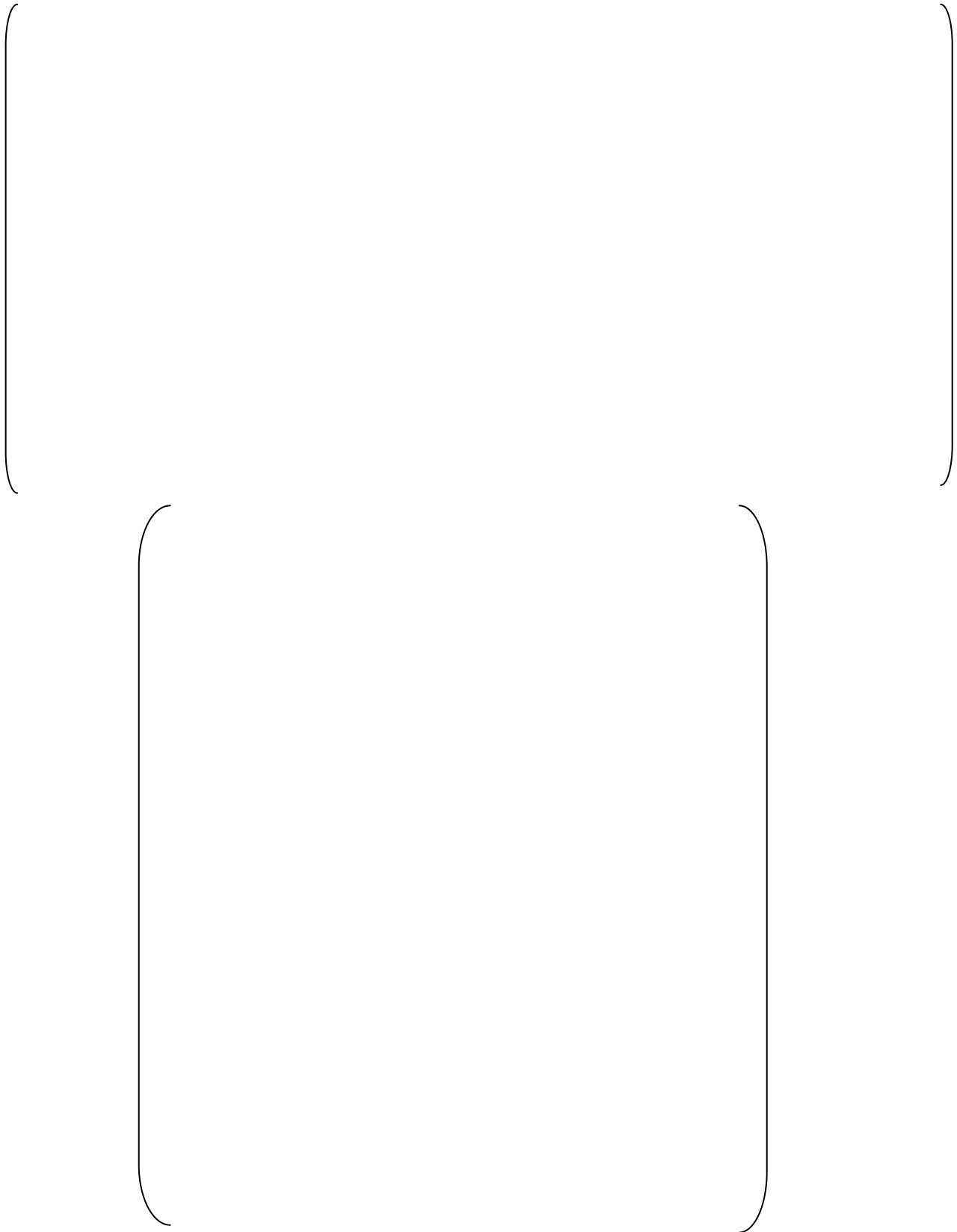


**Figure 2-9 Relation of Shear Force and Shear Strain**



**Figure 2-10 Crack Propagation (CA)**

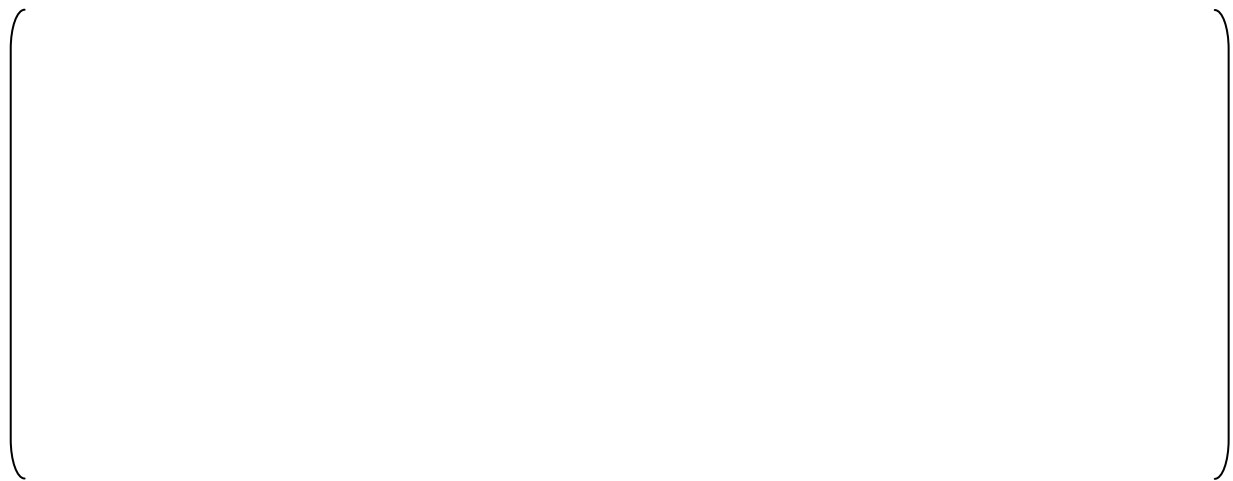


**Figure 2-11 Relation of b/t and Buckling Strain**



**Figure 2-12 Loading Method**



**Figure 2-13 Relation of Load and Displacement**

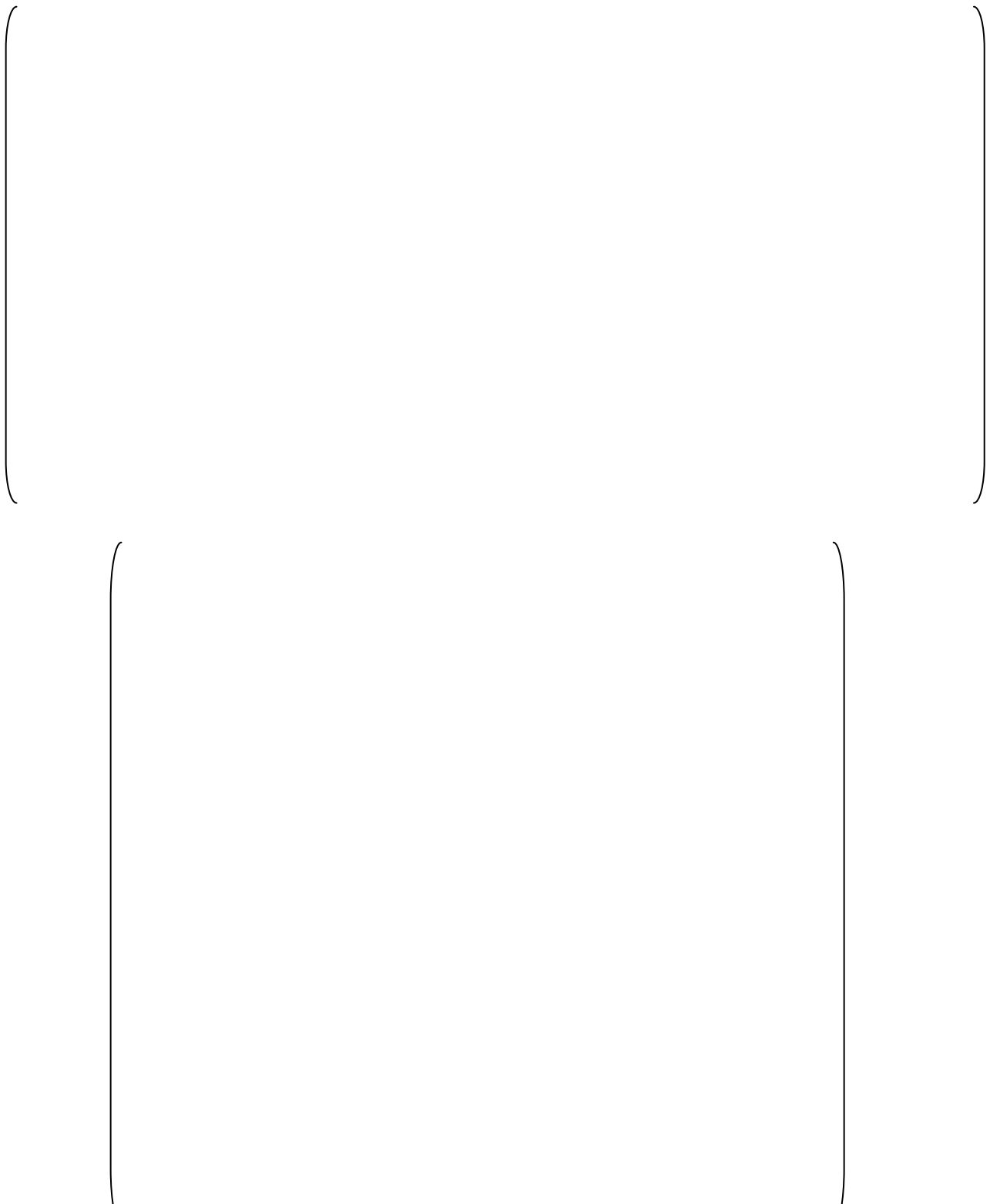


**Figure 2-14 A Sample of SC Design Recommendation**

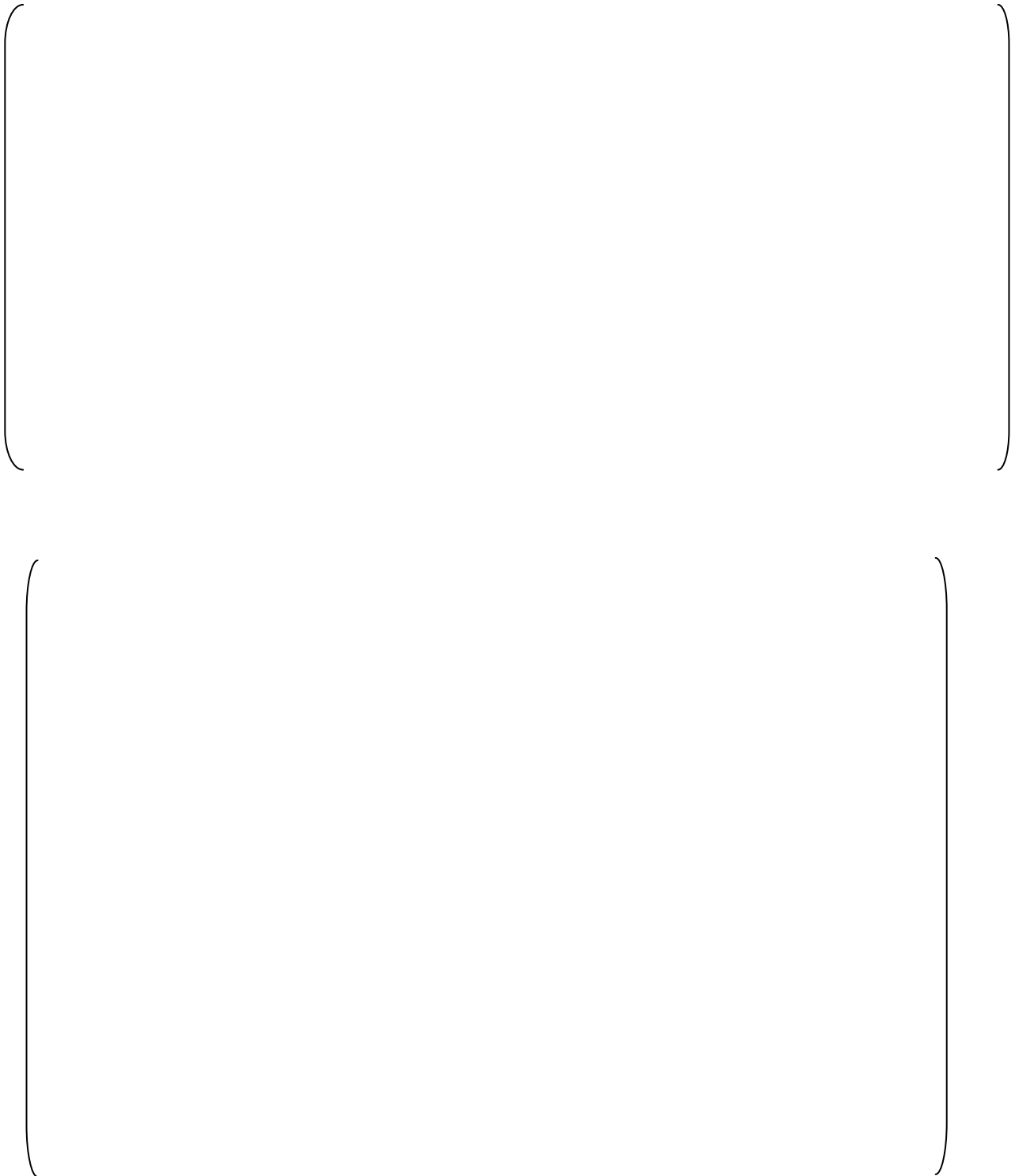


**Figure 2-15 Loading System of Pure Shear Force**



**Figure 2-16 Specimens of SC, Half SC and RC**

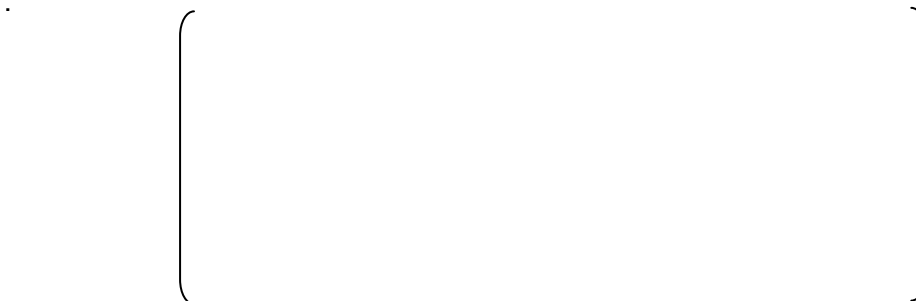


**Figure 2-17 Cracking of SC, Half SC and RC**

## **2.3 Overview of Experimental Database for SC Structure**

An overview of 12 references in the experimental database for SC composite structures are provided in Appendix A through D.

Appendix A provides an overview of the experimental database for SC composite that applies to the US-APWR, including a list of references applicable to the US-APWR, categories of US-APWR walls found in the CIS and their critical design parameters, and symbols and their definitions used throughout these appendices.

Appendix B focuses on the experimental database of SC beam out-of-plane shear tests and the test results are used to confirm the conservatism of the TeR MUAP-11019 Section 6.2 design equations for calculating the out-of-plane shear strength of SC walls.

Appendix C focuses on the experimental database of SC wall in-plane shear and the test results are used to confirm the conservatism of the TeR MUAP-11019 Section 7.3 design equation for calculating the in-plane shear strength of SC walls.

Appendix D focuses on the experimental database of axial compression tests conducted on SC walls and the local buckling behavior of steel faceplates. The experimental test results are used to confirm the conservatism of the TeR MUAP-11019 recommended maximum plate slenderness ratio of 20, and Section 2.2 design equation for calculating the axial compressive strength of SC walls.

### **3.0 STRENGTH EVALUATION OF US-APWR SC MODULES**

The SC modules of the US-APWR CIS are confirmed to have sufficient capacity and safety allowance to applied loads when designed using criteria based on ACI-349-06, based on the experimental results obtained by static loading tests of a 1/10<sup>th</sup> scale model of SC structures conducted by MHI, as described here.

#### **3.1 Methodology of the Evaluations**

To prove the integrity of the SC modules of the US-APWR CIS, the following comparisons between the SC modules of US-APWR CIS and that of the 1/10<sup>th</sup> scale model have been performed.

##### **(1) Comparison of Typical Dimensions**

The typical dimensions of the US-APWR CIS are evaluated by determining these dimensions from plan and section drawings for the SC modules, and comparing with the section dimensions in the 1/10<sup>th</sup> scale model. Since the SC module dimensions are approximately 10 times that of 1/10<sup>th</sup> scale model, it is confirmed that the dimensions of the test sections used in the 1/10<sup>th</sup> scale model are applicable.

##### **(2) Comparison of Sectional Properties**

The sectional properties, i.e. sectional area, moment of inertia and section modulus, of the US-APWR SC modules are compared to the sectional properties of the 1/10<sup>th</sup> scale model converted into real scale. Since the sectional properties of the SC modules are better than or equal to the converted properties from the 1/10<sup>th</sup> scale model, it is confirmed that the sectional properties of the test sections used in the 1/10<sup>th</sup> scale model are applicable.

##### **(3) Comparison of Ultimate Strength of Typical SC Wall Members**

The ultimate strengths of typical SC wall members used for the US-APWR SC modules are compared to the ultimate strengths of the 1/10<sup>th</sup> scale model converted into real scale. Since the ultimate strength of the SC modules are equal to or better than the converted ultimate strength from the 1/10<sup>th</sup> scale model, it is confirmed that the ultimate strength of the test sections used in the 1/10<sup>th</sup> scale model are applicable.

##### **(4) Safety Margin Against the Applied Design Forces of the US-APWR CIS**

The safety margins for the SC modules which comprise the US-APWR CIS are evaluated against the design forces applied to the US-APWR CIS, and ultimate strength capacity of the 1/10<sup>th</sup> scale model converted into real scale, and are determined to be acceptable. In addition, since the estimated capacity of the US-APWR CIS is greater than the ultimate strength capacity of the 1/10<sup>th</sup> scale model converted into real scale as evaluated in (2) and (3) above, the safety margin against the applied design forces of the US-APWR CIS is increased further.

## 3.2 Evaluation Results

### 3.2.1 Comparison of Typical Dimensions

The typical dimensions of the US-APWR CIS are evaluated as approximately 10 times that of the 1/10<sup>th</sup> scale model, by comparison of the dimensions on plan and section drawings for the SC modules.

Figure 3-1 and Table 3-1 compare the results of the typical dimensions. Figures 3-2 through 3-5 show the plans and the sections of SC modules used in the comparison between US-APWR and the 1/10<sup>th</sup> scale model.

- a) The comparison of typical dimensions of plans shows that the dimensions of the US-APWR CIS are nearly equal to the dimensions of the 1/10<sup>th</sup> scale model increased by a basic scale ratio of 10. The CIS dimensions exceed the dimensions of the 1/10<sup>th</sup> scale (times 10) except for the dimensions of secondary shield wall and pressurizer wall. It is judged that the strength reduction effect due to the differences of these walls to the overall ultimate strength of US-APWR CIS is insignificant. In this evaluation, the RWSP outer peripheral walls of the actual US-APWR CIS have been excluded to conservatively evaluate the total capacity of the structure.
- b) The comparison of typical thicknesses of the CIS walls shows that the thicknesses of the US-APWR are equal to or exceed the thicknesses of the 1/10<sup>th</sup> scale model increased by a basic scale ratio of 10, except the thickness of the pressurizer wall. It is judged that the strength reduction effect due to the difference of this wall to the overall ultimate strength of US-APWR CIS is insignificant.
- c) The comparison of typical heights of SC walls shows that the heights of US-APWR are approximately 1.5 times against the heights of 1/10<sup>th</sup> scale model increased by a basic scale ratio of 10. Therefore, it is judged that the bending moment applied to US-APWR CIS is larger than that to the real scale CIS converted from the 1/10<sup>th</sup> scale model. In the strength evaluation of US-APWR CIS, applied loads calculated for the US-APWR CIS design have been used.

Based on the above evaluations, it is concluded that the results of the 1/10<sup>th</sup> scale model test can be adopted to evaluate the strength capacity and safety allowance to applied loads of the US-APWR CIS with the basic scale ratio of 10.

--	--

**Table 3-1 Comparison of Dimensions**

--	--

**Security-Related Information - Withheld Under 10 CFR 2.390**

**Figure 3-2 Plan of SC Modules for US-APWR CIS**



**Security-Related Information – Withheld Under 10 CFR 2.390**

**Figure 3-3 Section of SC Modules for US-APWR CIS**

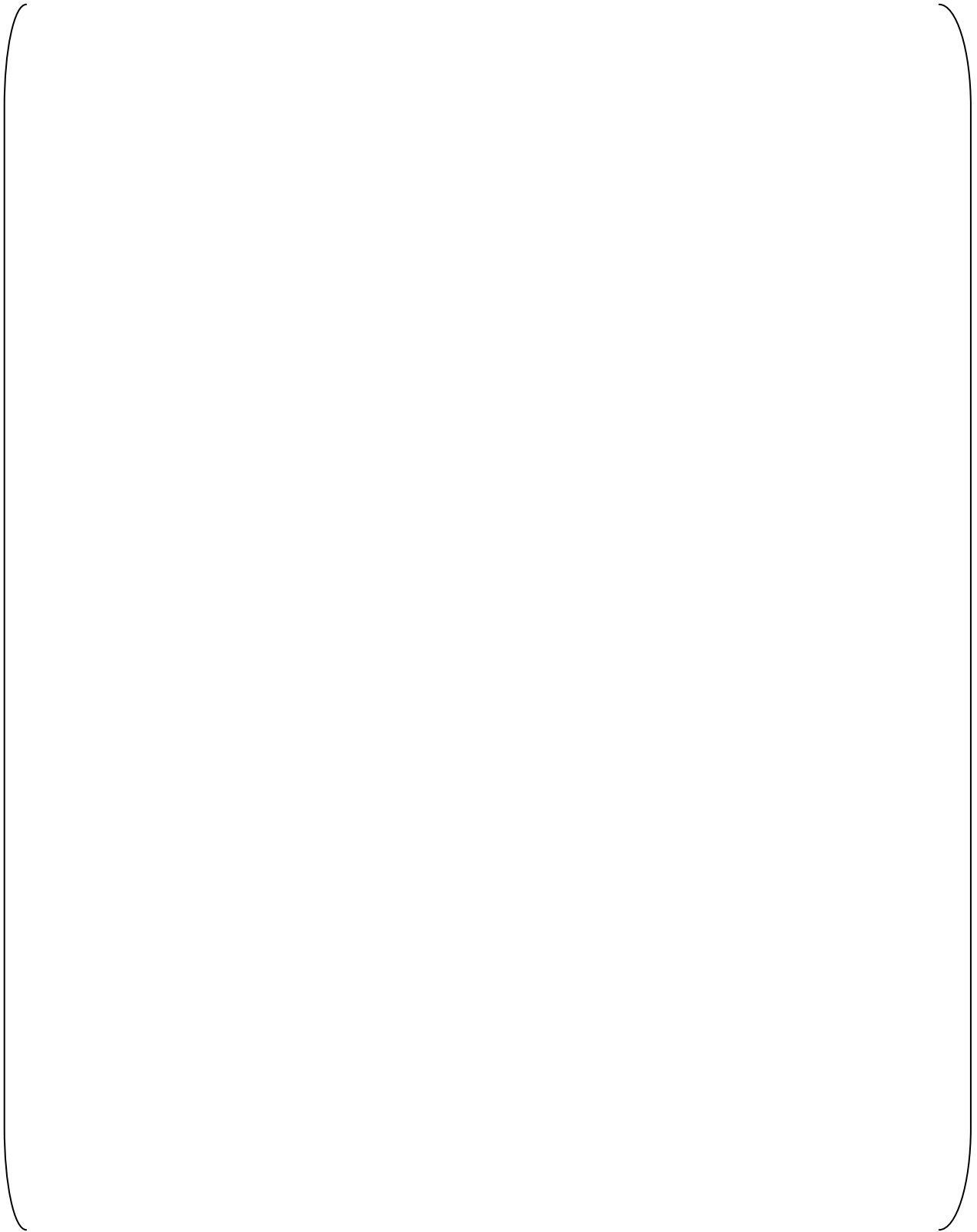


**Figure 3-4 SC Module Plan of 1/10<sup>th</sup> Scale Model**



**Figure 3-5 SC Module Section of 1/10<sup>th</sup> Scale Model**

### 3.2.2 Comparison of Sectional Properties

The sectional properties, i.e. sectional area, moment of inertia and section modulus, of the US-APWR CIS are evaluated as greater than or equal to the properties of the 1/10<sup>th</sup> scale model converted to real scale, by comparing these properties for SC modules.

#### (1) Basis of the Evaluation

- a) In the calculation of the sectional properties of the SC module, only the concrete sectional area has been taken into account except for the steel sectional area.
- b) The sectional properties of the overall CIS are calculated based on the results of the calculation of the sectional properties for each SC module wall members.
- c) The sectional properties of the 1/10<sup>th</sup> scale model are converted into real scale using a basic scale ratio of 10, for comparison with the properties of the US-APWR CIS. Sectional area, moment of inertia and section modulus are calculated as 100 times, 10,000 times and 1,000 times of original values of the 1/10<sup>th</sup> scale model, respectively.

#### (2) Results

Figure 3-6 and Table 3-2 show the results of the evaluation using the above basis. Figures 3-7 and 3-8 show the overview plans of US-APWR and 1/10<sup>th</sup> scale model used in this evaluation.

It is verified that the sectional properties of US-APWR are greater than or equal to those of the 1/10<sup>th</sup> scale model converted into real scale, because the ratio (a/b) of sectional properties exceeds 1.0 as shown in Figure 3-6.

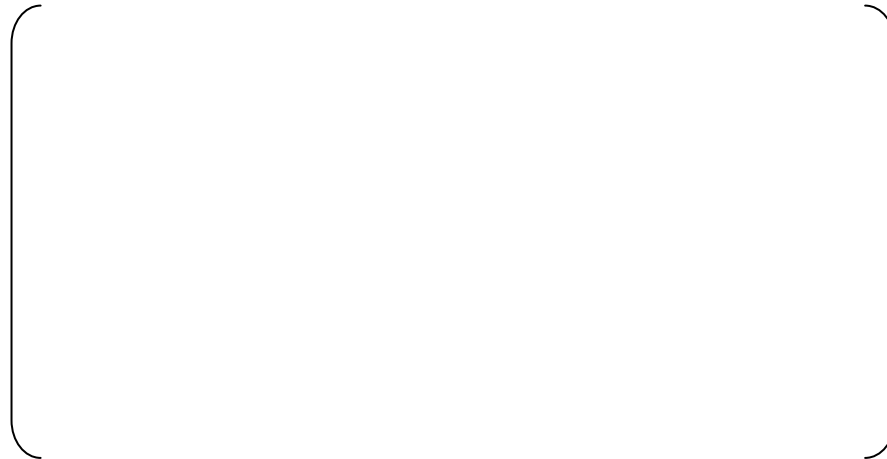


**Figure 3-6 Comparison of Sectional Properties**

**Table 3-2 Comparison of Sectional Properties**

--	--



**Figure 3-7 Overview Plan of US-APWR**



**Figure 3-8 Overview Plan of 1/10<sup>th</sup> Scale Model**

### 3.2.3 Comparison of Ultimate Strength of SC Wall Members

The ultimate strengths of typical SC wall members used for the US-APWR SC modules are compared to the ultimate strengths of the 1/10<sup>th</sup> scale model converted into real scale, and determined to be equal to or better than the converted ultimate strength from the 1/10<sup>th</sup> scale model.

#### (1) Calculation methodology

The ultimate strengths for SC module wall members are calculated using JEAC 4618-2009, "Technical Code for Seismic Design of Steel Plate Reinforced Concrete Structures".

Table 3-3 shows the material properties of the SC modules. The yield strength of steel and the compression strength of concrete are the values obtained by test of the 1/10<sup>th</sup> scale model, and the values specified in the design specification for the US-APWR.

Figure 3-9 shows the structural overviews of SC module wall members for US-APWR and the 1/10<sup>th</sup> scale model. The ultimate strengths of the 1/10<sup>th</sup> scale model are converted into real scale based on the basic scale ratio of 10, for comparison with those of the US-APWR.

#### (2) Calculation results

Figure 3-10 and Table 3-4 show the comparison of the ultimate strengths of SC module wall members for the US-APWR and the 1/10<sup>th</sup> scale model.

It is verified that the ultimate strengths of the SC module wall member for US-APWR are greater than those of the 1/10<sup>th</sup> scale model converted into real scale, because the ratios (a/b) of strengths exceed 1.0 as shown in Figure 3-10.

**Table 3-3 Material Properties of SC Modules**



**Figure 3-9 Overview of SC Modules Wall Member**



**Table 3-4 Comparison of SC Wall Member Strengths**



### 3.2.4 Safety Margin Against the Design Applied Forces of US-APWR CIS

The safety margins for the design forces applied to the US-APWR CIS are evaluated as acceptable against the ultimate strength capacity of the 1/10<sup>th</sup> scale model converted into real scale. In addition, the actual safety margins of the estimated capacity of the US-APWR CIS, considering the evaluation in 3.2.2 and 3.2.3 above, is evaluated to provide even greater margin.

#### (1) Evaluation Methodology

Figure 3-11 shows the load-displacement curve obtained by the static loading test of the 1/10<sup>th</sup> scale model. The maximum force is 11.49MN, and the failure mode is shear failure. The loading points of the test are at two levels. The maximum forces are distributed with 8.29MN on the upper point whose height is 1490mm from the base, and 3.20MN on the lower point at a height of 730mm from the base. The ultimate shear force and bending moment are calculated by the maximum force.

Figure 3-12 shows the distributions of shear force and bending moment calculated for the governing cases in SC modules of the US-APWR. The maximum design shear force and bending moment are produced by these distributions.

The ultimate shear force and bending moment of the 1/10<sup>th</sup> scale model are converted into real scale based on the basic scale ratio of 10, for the comparison with sections of the US-APWR CIS. The safety margins of the ultimate capacities of the 1/10<sup>th</sup> scale model converted into real scale for the design forces of the US-APWR CIS are evaluated by comparison. In addition, actual ultimate shear and bending moment capacities of the SC modules in the US-APWR CIS are estimated based on the evaluation of sectional properties listed in Table 3-2 and ultimate strengths of SC wall members listed in Table 3-4. For these estimated capacities, the safety margins have been evaluated.

#### (2) Results of the Evaluations

Figure 3-13, Table 3-5 and Table 3-7 show the safety margins against the maximum design forces of the US-APWR CIS. Table 3-6 shows the results of the calculated estimated ultimate capacities of SC modules for the US-APWR CIS.

Results of the evaluations are as follows:

- It is verified that, based on the 1/10<sup>th</sup> scale model test to the maximum design shear force, the margin is 5.2 for the ultimate strength capacity of SC modules in the US-APWR CIS, and 3.3 for the maximum design bending moment.
- It is verified that, for the estimated ultimate strength capacities of SC modules in the US-APWR CIS, the margin is 8.9 for the maximum design shear force and 6.2 for the maximum design bending moment.
- The margin for bending moment is less than that for the shear force. Therefore it is determined that the margin for bending moment exceeds 6.2, because the 1/10<sup>th</sup> scale model failed by shear force and not by bending moment.



**Figure 3-11 Load-Displacement Curve of 1/10<sup>th</sup> Scale Model**

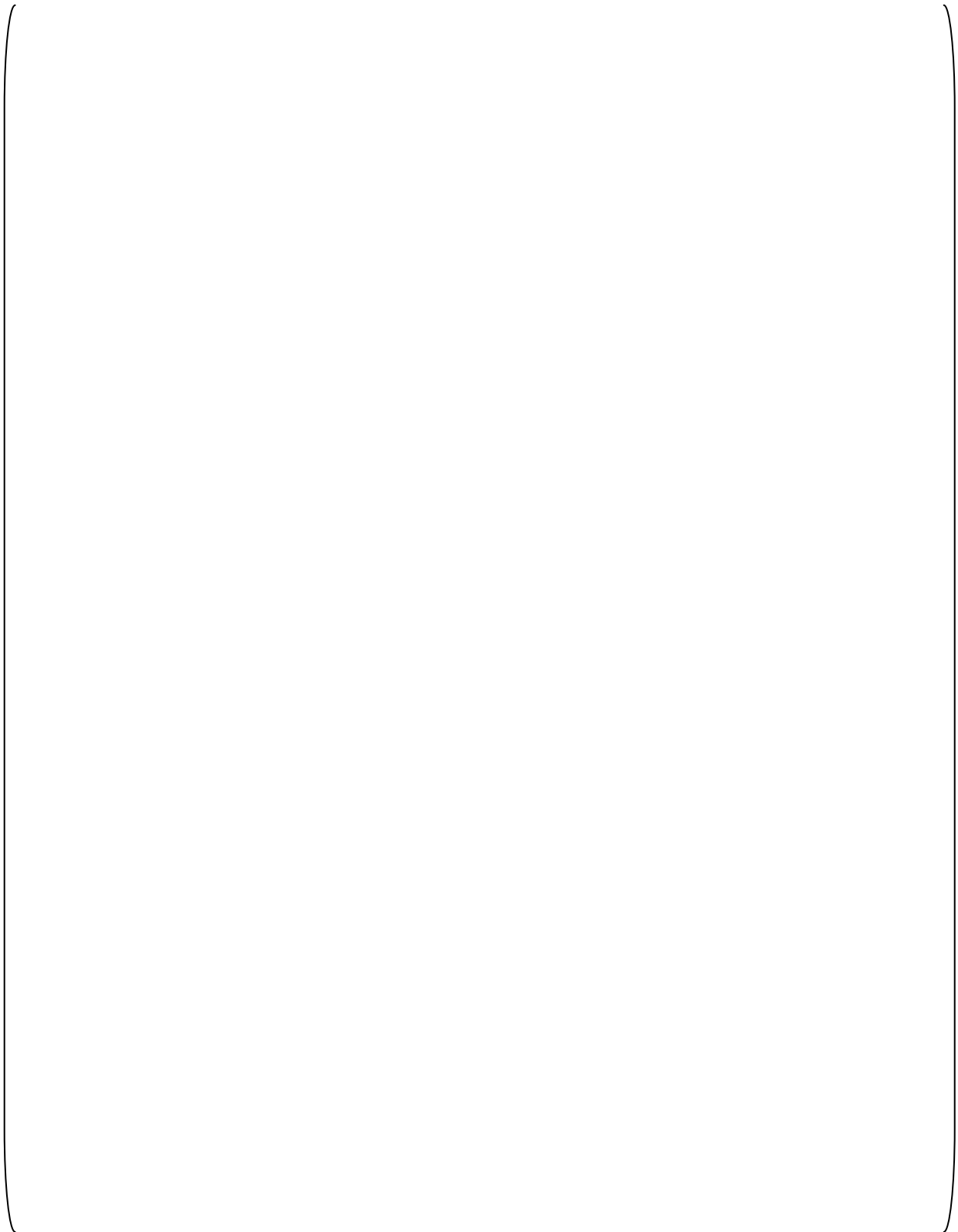


**Figure 3-12 Distribution of Design Shear Force and Bending Moment  
for the US-APWR**



**Table 3-5 Margin for Design Force of the US-APWR (1)**



**Table 3-6 Estimated Ultimate Capacity of SC Modules in the US-APWR CIS**

--

**Table 3-7 Margin for Design Force of the US-APWR (2)**

--

## 4.0 CONCLUSION

### 4.1 Research Achievements

Revision 0 of this TeR introduced the 10 research achievements for SC modules. In addition, this TeR has shown that the SC modules of the US-APWR CIS, when designed using criteria based on ACI-349-06, has enough strength capacity and safety allowance to applied loads, based on the experimental results obtained by static loading test of the 1/10<sup>th</sup> scale model of SC modules. The design criteria are further described in TeRs MUAP-11013, MUAP-11019, and MUAP-11020.

The following conclusions summarize the evaluation results of US-APWR SC modules:

- a) The strength evaluation of the SC modules in the US-APWR CIS is conservative based on the 1/10<sup>th</sup> scale model test results using the basic scaling ratio of 10.
- b) The sectional properties of the US-APWR are greater than or equal to that of the 1/10<sup>th</sup> scale model converted into real scale.
- c) The ultimate strengths of the US-APWR wall members are greater than that of the 1/10<sup>th</sup> scale model converted into real scale.
- d) The safety margins of the SC modules in the US-APWR CIS are 8.9 for maximum design shear force and 6.2 for the maximum design bending moment.

Based on the evaluations mentioned above, it is confirmed that the SC modules in the US-APWR CIS have sufficient safety margins to the design forces.

### 4.2 Experimental Database

Revision 1 of this TeR adds an overview of the experimental database for SC composite structures that applies to the US-APWR.

The following conclusions summarize the evaluation of the experimental database presented in Appendix A through D:

- a) The TeR MUAP-11019 Section 6.2 design equations are conservative for calculating the out-of-plane shear strength of SC walls.
- b) The TeR MUAP-11019 Section 7.3 design equation is conservative for calculating the in-plane shear strength of SC walls.
- c) The TeR MUAP-11019 Section 2.2 design equation is conservative for calculating the axial compressive strength of SC walls with the TeR MUAP-11019 recommended maximum plate slenderness ratio of 20.

## 5.0 REFERENCES

1. Takeuchi, M; et al; "Experimental Study on Steel Plate Reinforced Concrete Structure Part 28 Response of SC Members Subjected to Out-of-plane Load (Outline of the Experimental Program and the Results)", Papers 2619 and 2620, Summaries of Technical Papers of Annual Meeting, Architectural Institute of Japan, 1999
2. Hong, S; et al; (2009) "Out-of-Plane Shear Strength of Steel Plate Concrete Walls Dependent on Bond Behavior", SMiRT-20, Div-6: Paper ID# 1855, 9-14, Espoo, Finland, August, 2011
3. Varma, A.H.; Sener, K.C.; Zhang, K.; Coogler, K; and Malushte, S.R.; (2011). "Out-of-Plane Shear Behavior of SC Composite Structures." Trans. of the Internal Assoc. for Struct. Mech. in Reactor Tech. Conf., SMiRT-21, Div-VI: Paper ID# 763, 6-11, New Delhi, India, November, 2011
4. Akiyama, H; et al; "1/10<sup>th</sup> Scale Model Test of Inner Concrete Structure Composed of Concrete Filled Steel Bearing Wall", Annual Conference of Architectural Institute of Japan, 2003 (Parts 1-3, pp. 1027- 1031)
5. Akita, S; et al; "A Study on the Structural Performance of SC Thick Walls Part 1 Experiment of the SC Thick Wall", 1989, SMiRT#10, pp. 73-78
6. Akita, S; et al; "Experiment for Fire Resistance of A Concrete Filled Steel Structure Part 1. Bearing Wall (Outline of experimental program and the results)", Annual Conference of Architectural Institute of Japan, 1997 (pp. 171-174)
7. Kanchi, M; et al; "Experiment for Fire Resistance of a Concrete Filled Steel Structure Part 6 Bearing Wall (The Estimation of Influence on Specification Structure: Planning of Experimental and Results)", Annual Conference of Architectural Institute of Japan, 1999
8. Sekimoto, H; et al; "Study on Property of Concrete-filled Steel-bearing Wall Subjected to High Temperature", Journal of Structural Engineering. B, VOL.47B, pp481-490, 2001
9. Sekimoto, H; et al; "Experimental Study on Property of SC Structure Subjected to High Temperature Hysteresis", Journal of Structural Engineering. B, VOL.49B, pp391-399, 2003
10. Funakoshi, A.; Akita, S.; Matsumoto, H.; Hara, K., Matsuo, I.; and Hayashi, N. "Experimental Study on A Concrete Filled Steel Structure Part. 7 Bending Shear Tests (Outline of the experimental program and the results)", Summaries of Technical Papers of Annual Meeting, Architectural Institute of Japan, 1998, pp. 1063-1064
11. Fujita, T.; Funakoshi, A.; Akita, S.; Hayashi, N.; Matsuo, I.; and Yamaya, H. "Experimental Study on A Concrete Filled Steel Structure Part. 16 Bending Shear Tests (Effect of Bending Strength)", Summaries of Technical Papers of Annual Meeting, Architectural Institute of Japan, 1998, pp. 1125-1126

12. Kitano, T.; Akita, S., Nakazawa, M.; Fujino, Y.; Ohta, H.; Yamaguchi, T.; Nakayama, T.;  
“Experimental Study on a Concrete-filled Steel Structure Part 4: Shear Tests (Outline of  
the experimental program and the results)”, Summaries of Technical Papers of Annual  
Meeting, Architectural Institute of Japan. B-2, pp. 1057-1058, 1997
13. Ozaki, M., Akita, S., Takeuchi, M.; et al, “Experimental Study on Steel-plate-reinforced  
Concrete Structure,  
Part. 41 Heating Tests (Outline of Experimental Program and Results),  
Part. 42 Heating Tests (Thermal Deformation Behavior),  
Part. 43 Heating Tests (Mechanical Aspects of SC Panels after Heating)”,  
Summaries of Technical Papers of Annual Meeting, Architectural Institute of Japan,  
2000, pp. 1127-1132
14. Usami, S.; Akiyama, H., Narikawa, M.; Hara, K.; Takeuchi, M.; and Sasaki, N.; "Study  
on a concrete filled steel structure for nuclear power plants (part 2). Compressive  
loading tests on wall members", SMiRT-13, Porto Alegre, Brazil, August, 1995
15. Kanchi, M.; et al, "Experimental Study on Concrete-filled Steel Structure: Part 2  
Compressive Tests Characteristics Test (1)", Summaries of technical papers of Annual  
Meeting Architectural Institute of Japan. B-2, Structures II, Structural dynamics nuclear  
power plants 1996, 1071-1072, 1996-07-30
16. Sekimoto, H., "Experimental Study on Concrete Filled Steel Shear Wall: Part 1  
Compression Test of Seismic Wall", Summaries of technical papers of Annual Meeting  
Architectural Institute of Japan. Structures II 1991, 1659-1660, 1991-08-01
17. Akita, S; Ozaki, M; “Earthquake-Resistant Design Recommendation for Building Using  
Steel Plate Reinforced Concrete Structure (Design Method of Earthquake-Resistant  
Wall)”, Technical Report of Architectural Institute of Japan, Dec., 2001, No.14,  
pp123-128
18. Ozaki, M. et al, “Study on Steel Plate Reinforced Concrete Panels Subjected to Cyclic  
In-Plane Shear”, Nuclear Engineering and Design, Volume 228, 2004
19. Varma, A.; Malushte, S.; Sener, K.; Both, P.; Coogler, K.; “Steel-Plate Composite (SC)  
Walls: Analysis and Design Including Thermal Effects”, SMiRT 21, New Delhi, India,  
November 2011

The full research reports of these references are provided in Appendix E.

# **Appendix A**

## **Experimental Database and US-APWR SC Wall Design**

## **APPENDIX A**

### **TABLE OF CONTENTS**

Appendix A Experimental Database and US-APWR SC Wall Design .....	A-1
---	-----

### **LIST OF TABLES**

Table A-1 SC Experimental Database References .....	A-1
Table A-2 US-APWR Category 1 and 2 SC Walls Categorization by Steel Reinforcement Ratio ( $2t_p/T$ ) .....	A-4
Table A-3 Definition of Symbols Used in Experimental Database .....	A-5

## Experimental Database and US-APWR SC Wall Design

This Appendix provides an overview of the experimental database for SC composite walls that applies to the US-APWR. Appendices B through D to the TeR MUAP-11005 further present and discusses the significance of the research database. Appendix A provides a list of references applicable to the US-APWR (Table A-1), categories of US-APWR walls found in the CIS and their critical design parameters (Table A-2), and symbols and their definitions used throughout these appendices (Table A-3).

Table A-1 includes the details of the papers used to compile the experimental database of tests conducted on SC walls. It includes: (i) reference number that is used as the identifier to cite these references in the appendices, (ii) the title and author(s) of the reference. These references are included in Appendix E.

**Table A-1 SC Experimental Database References**

No.	Reference Title
[1]	Takeuchi, M; et al; "Experimental Study on Steel Plate Reinforced Concrete Structure Part 28 Response of SC Members Subjected to Out-of-plane Load (Outline of the Experimental Program and the Results)", Papers 2619 and 2620, Summaries of Technical Papers of Annual Meeting, Architectural Institute of Japan, 1999
[2]	Hong, S; et al; (2009) "Out-of-Plane Shear Strength of Steel Plate Concrete Walls Dependent on Bond Behavior", SMiRT-20, Div-6: Paper ID# 1855, 9-14, Espoo, Finland, August, 2011
[3]	Varma, A.H.; Sener, K.C.; Zhang, K.; Coogler, K; and Malushte, S.R.; (2011). "Out-of-Plane Shear Behavior of SC Composite Structures." Trans. of the Internal Assoc. for Struct. Mech. in Reactor Tech. Conf., SMiRT-21, Div-VI: Paper ID# 763, 6-11, New Delhi, India, November, 2011
[8]	Sekimoto, H; et al; "Study on Property of Concrete-filled Steel-bearing Wall Subjected to High Temperature", Journal of Structural Engineering. B, VOL.47B, pp481-490, 2001
[9]	Sekimoto, H; et al; "Experimental Study on Property of SC Structure Subjected to High Temperature Hysteresis", Journal of Structural Engineering. B, VOL.49B, pp391-399, 2003
[10]	Funakoshi, A.; Akita, S.; Matsumoto, H.; Hara, K., Matsuo, I.; and Hayashi, N. "Experimental Study on A Concrete Filled Steel Structure Part. 7 Bending Shear Tests (Outline of the experimental program and the results)", Summaries of Technical Papers of Annual Meeting, Architectural Institute of Japan, 1998, pp. 1063-1068
[11]	Fujita, T.; Funakoshi, A.; Akita, S.; Hayashi, N.; Matsuo, I.; and Yamaya, H. "Experimental Study on A Concrete Filled Steel Structure Part. 16 Bending Shear Tests (Effect of Bending Strength)", Summaries of Technical Papers of Annual Meeting, Architectural Institute of Japan, 1998, pp. 1121-1128
[12]	Kitano, T.; Akita, S., Nakazawa, M.; Fujino, Y.; Ohta, H.; Yamaguchi, T.; Nakayama, T.; "Experimental Study on a Concrete-filled Steel Structure Part 4: Shear Tests (Outline of the experimental program and the results)", Summaries of Technical Papers of Annual Meeting, Architectural Institute of Japan. B-2, pp. 1057-1058, 1997

- [13] Ozaki, M., Akita, S., Takeuchi, M.; et al, "Experimental Study on Steel-plate-reinforced Concrete Structure Part. 41 Heating Tests (Outline of Experimental Program and Results), Part. 42 Heating Tests (Thermal Deformation Behavior), Part. 43 Heating Tests (Mechanical Aspects of SC Panels after Heating)", Summaries of Technical Papers of Annual Meeting, Architectural Institute of Japan, 2000, pp. 1131-1132
- [14] Usami, S.; Akiyama, H., Narikawa, M.; Hara, K.; Takeuchi, M.; and Sasaki, N.; "Study on a concrete filled steel structure for nuclear power plants (part 2). Compressive loading tests on wall members", SMiRT-13, Porto Alegre, Brazil, August, 1995
- [15] Kanchi, M.; et al, "Experimental Study on Concrete-filled Steel Structure: Part 2 Compressive Tests Characteristics Test (1)", Summaries of technical papers of Annual Meeting Architectural Institute of Japan. B-2, Structures II, Structural dynamics nuclear power plants 1996, 1071-1072, 1996-07-30
- [16] Sekimoto, H., "Experimental Study on Concrete Filled Steel Shear Wall: Part 1 Compression Test of Seismic Wall", Summaries of technical papers of Annual Meeting Architectural Institute of Japan. Structures II 1991, 1659-1660, 1991-08-01

\*The full research reports of these references are provided in Appendix E

As explained in the TeR MUAP-11019, the US-APWR SC wall design philosophy prevents SC specific failure modes from governing the design. These SC specific failure modes include:

- i. Local buckling of the steel faceplates prior to yielding in compression.
- ii. Interfacial shear failure prior to out-of-plane shear failure.
- iii. Delamination or splitting failure of SC walls through the concrete thickness

These failure modes are prevented by detailing the SC wall sections with adequate shear studs (size and spacing) and tie system (size and spacing) to achieve:

- i. Steel faceplate slenderness ( $s/t_p$ ) ratio less than or equal to 20 as described in TeR MUAP-11019 Section 2.2
- ii. Development lengths ( $L_d$ ) less than or equal to two times the SC wall thickness as described in TeR MUAP-11019 Section 2.4
- iii. Interfacial shear strength greater than or equal to the out-of-plane shear strength ( $V_{no}$ ) as described in TeR MUAP-11019 Section 2.5
- iv. Tie system spacing and strength to prevent postulated delamination or splitting failure as described in TeR MUAP-11019 Section 2.6.

Additionally, the SC walls of the US-APWR CIS are designed and detailed with tie systems (size and spacing) such that flexural yielding of the steel faceplates will occur prior to out-of-plane shear failure ( $V_{no}$ ) for shear span ratios greater than or equal to 2.0. The resulting tie systems consist of: (i) rectangular bars made from A572 Gr.50 steel, with (ii) spacing less than or equal to the wall thickness divided by two.

Table A-2 presents relevant details of the SC walls in the US-APWR CIS. The walls are categorized by the steel reinforcement ratio category (SRRC). The SRRC is the most important parameter given the fact that all other parameters, namely, shear stud and tie system size and spacing, have been designed and detailed as described above to prevent SC specific failure modes (local buckling, interfacial shear failure, and section delamination) from governing the design, and to prevent out-of-plane shear failure from occurring before flexural yielding for shear span ( $a/d$ ) ratios greater than or equal to 2.0.

**Table A-2 US-APWR Category 1 and 2 SC Walls Categorization by Steel Reinforcement Ratio ( $2t_p/T$ )**

--	--

The experimental databases presented in Appendix A through D use the SRRC to relate the tested specimens to the US-APWR SC walls. The tested specimens typically fail with failure modes that are prevented for the US-APWR SC walls through appropriate design and detailing of the shear studs and tie systems. Therefore, the test results in the experimental database are appropriate for verifying the conservatism of the SC wall design equations used in TeR MUAP-11019. These test results do not necessarily show the behavior of the US-APWR SC walls because those are detailed to provide better overall performance and ductility by preventing SC specific failure modes etc. as described earlier.

The symbols used to identify geometric and material parameters for the tested specimens are defined in Table A-3

**Table A-3 Definition of Symbols Used in Experimental Database**

T	wall thickness in mm
$t_p$	steel plate thickness in mm
$t_c$	concrete thickness in mm
$\rho$	steel reinforcement ratio = $2t_p/T$
B	specimen width in mm
H	specimen height in mm
a	shear span length in mm
$d_{stud}$	diameter of shear stud in mm
$l_{stud}$	length of shear stud in mm
$a_{stud}$	cross-sectional area of stud in mm <sup>2</sup>
$s_{stud}$	spacing of shear stud in mm
$\rho_{stud}$	shear stud reinforcement ratio, = $a_{stud}/s_{stud}^2$
$d_{tie}$	diameter of tie bar in mm
$s_{tie}$	spacing of tie bar in mm
$a_{tie}$	cross-sectional area of tie bar in mm <sup>2</sup>
$\rho_{tie}$	tie bar reinforcement ratio, = $a_{tie}/s_{tie}^2$
$f_{y\_plate}$	yield strength of steel plate in MPa
$f_{u\_plate}$	ultimate strength of steel plate in MPa
$f_{y\_stud}$	yield strength of shear stud in MPa
$f_{u\_stud}$	ultimate strength of shear stud in MPa
$f_{y\_tie}$	yield strength of tie bar in MPa
$f_{u\_tie}$	ultimate strength of tie bar in MPa
$f'_c$	cylinder compressive strength of concrete in MPa

## **Appendix B**

### **Out-of-Plane Experimental Database and Comparison with Design Equation**

## APPENDIX B

### TABLE OF CONTENTS

Appendix B Out-of-Plane Experimental Database and Comparison with Design Equation .....	B-1
--	-----

### LIST OF FIGURES

Figure B-1 Experimental Results Comparisons with TeR MUAP-11019 Section 6.2 Shear Strength Equations (Eq 6.2-1 + Eq 6.2.-4).....	B-6
Figure B-2 Experimental Results Comparisons with TeR MUAP-11019 Section 6.2 Shear Strength Equations (Eq 6.2-1 + Eq 6.2.-4).....	B-7
Figure B-3 Experimental Results Comparisons with TeR MUAP-11019 Section 6.2 Concrete Shear Strength Equations (Eq 6.2-1).....	B-9

### LIST OF TABLES

Table B-1 Japanese Out-of-Plane Shear Tests (Reference 1) .....	B-2
Table B-2 Korean Out-of-Plane Shear Tests (Reference 2) .....	B-3
Table B-3 Purdue Out-of-Plane Shear Tests (Reference 3) .....	B-4

### **Out-of-Plane Experimental Database and Comparison with Design Equation**

This Appendix focuses on the experimental database of out-of-plane shear tests conducted in Japan, Korea, and US. The experimental database of SC beam out-of-plane shear tests is presented, and the test results are used to confirm the conservatism of the TeR MUAP-11019 Section 6.2 design equations for calculating the out-of-plane shear strength of SC walls.

The US-APWR SC walls are designed with adequate tie bar size and spacing to enable flexural yielding of the steel faceplates, and prevent out-of-plane shear failure from governing the strength for shear span ratios greater than 2.0.

Table B-1, Table B-2 and Table B-3 present the experimental database of out-of-plane shear tests conducted in Japan, South Korea, and the US, respectively. These tables represent the test database of out-of-plane shear tests conducted by means of testing beam specimens. SC beam specimens having combinations of shear studs, shear reinforcement bars, and stiffener sections (ribs) that are anchored into the concrete infill have been tested under different out-of-plane loading configurations. The parameters used in these tests were: shear span-to-depth ratios, steel plate reinforcement ratios, stud and tie bars reinforcement ratios.

In total, 29 beam tests have been conducted to investigate the out-of-plane behavior under combined shear and flexural loading. The bottom of each table in this Appendix B includes the loading patterns (a), (b), (c), and (d) that have been used to conduct the experiments. 'Loading type a' is a two-point support four-point loading configuration, and 'Loading type c' is an anti-symmetric loading configuration. These loadings simulate fixity at support locations, and the shear span-to-depth ratio is calculated by taking the ratio of moment and shear at the section where they are maximum and dividing it by the section depth ( $M_u/V_u d$ ). Loading Types 'b' and 'd' are simple three and four point bending configurations and the shear span is measured by the distance from the load point to the nearest support.

**Table B-1 Japanese Out-of-Plane Shear Tests (Reference 1)**

--	--

**Table B-2 Korean Out-of-Plane Shear Tests (Reference 2)**

--	--

**Table B-3 Purdue Out-of-Plane Shear Tests (Reference 3)**

Japanese researchers have tested 16 SC beams that had combinations of shear studs and round tie bars anchored to concrete. Most of the specimens had shear span-to-depth ratios less than 1.5, with the exception of three specimens. The section depths were within the range from 8 in. to 24 in., or 203 mm to 609 mm. The steel faceplate reinforcement ratios varied from 1.33% to 4%, calculated based on the total steel area in the cross-section. The composite action factor (plate slenderness) which is defined as shear stud spacing to steel plate thickness ( $s_{stud}/t_p$ ), varied from 22 to 44. The mechanical properties of steel and concrete used in these tests closely reflect the material properties that are specified in the actual design of US-APWR SC walls. Loading configurations 'a', 'b', and 'c' were used for testing the beams. The experimental program included 6 specimens (#8, #9, #10, S3, S4, S5, S6) having shear reinforcement out of total of 16 specimens. The geometric details for the specimens are given in Table B-1.

Specimen #7 had steel reinforcement ratios ( $2t_p/T$ ) of 1.33%. This is within the range (1-2%) of the US-APWR Steel Reinforcement Ratio Category-1 (SRRC-1), and corresponds to US-APWR Section IDs 107 (refueling/reactor cavity walls) and 108 (north refueling cavity walls) as shown in Table A-2.

Specimens #2, #3, #4, #5, and #6 had steel reinforcement ratios ( $2t_p/T$ ) of 2.0%. This is within the range (2-2.5%) of the US-APWR Steel Reinforcement Ratio Category-2 (SRRC-2), and corresponds to US-APWR Section IDs 103 (south reactor cavity walls) and 104 (secondary shield walls) as shown in Table A-2.

Specimens S1, S2, S3, S4, S5, and S6 had steel reinforcement ratios ( $2t_p/T$ ) of 3.6%. This is within the range (3-4%) of the US-APWR Steel Reinforcement Ratio Category-4 (SRRC-4), and corresponds to US-APWR Section ID 105 (lower pressurizer walls) as shown in Table A-2.

Similarly, Specimens #1, #8, #9 and #10 had steel reinforcement ratios ( $2t_p/T$ ) of 4.0%. This is within the range (4-5%) of the US-APWR Steel Reinforcement Ratio Category-5 (SRRC-5), and corresponds to US-APWR Section IDs 106 (mid-height pressurizer walls) as shown in Table A-2.

As indicated earlier, all 16 specimens had plate slenderness ratios ( $s/t_p$ ), ranging from 20.8 to 30. This plate slenderness is larger than the  $s/t_p$  ratios (8 – 16) for US-APWR SC wall design for all Section IDs as shown in Table A-2. The specimens with shear reinforcement had similar shear reinforcement spacing to section depth ratios ( $s_{tie}/T$ ). Specimens #9 and #10 had  $s_{tie}/T$  of 0.42 where the corresponding US-APWR Section 106 had 0.50. Furthermore, Specimens S3, S4, S5 and S6 had  $s_{tie}/T$  of 0.5 that is the identical ratio of the corresponding US-APWR section 105. Additionally, 10 of the specimens did not have any tie bars or connectivity between the two opposite steel faceplates.

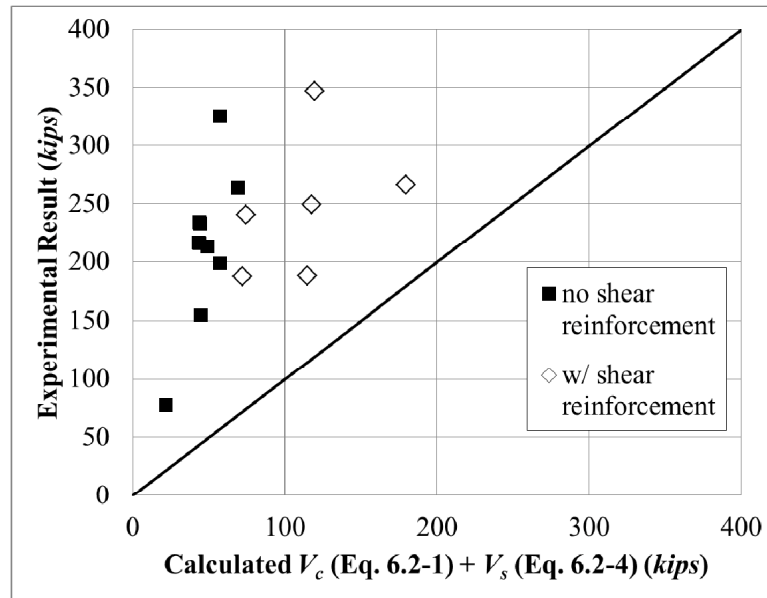


**Figure B-1 Experimental Results Comparisons with TeR MUAP-11019 Section 6.2 Shear Strength Equations (Eq 6.2-1 + Eq 6.2-4)**

Figure B-1 shows comparisons of the experimental results for the 16 specimens including those both with and without shear reinforcement and compared calculated using summation of Equations 6.2-1 and 6.2-4 of TeR MUAP-11019. The comparison indicates that the shear strength is estimated conservatively by the design equation for all the specimens. The US-APWR SC walls have closely spaced rectangular tie bars. The behavior and ductility of the US-APWR SC walls will be better than those of the specimens that did not have any shear reinforcement. Nevertheless, the design strengths for out-of-plane shear can be estimated conservatively using TeR MUAP-11019 design equations.

Korean researchers also did similar testing where they tested 13 specimens having combinations of shear studs, tie bars and welded plate stiffeners sections (ribs) anchored into concrete. Specimens with names beginning with NR did not have any plate stiffener members and shear span-to-depth ratios were on the low side by being 1.6 and 2. The reinforcement ratios were in the range of 2.25 to 4.5%. The remainder of the specimens with names beginning with B or S had relatively larger shear span-to-depth ratios as being 3.6 in both loading configurations 'b' and 'c'. In these specimens the influence of stiffener members (ribs) that are continuously welded to the inner faces of the steel plates in the longitudinal direction were also studied. The section depths were in the range of 15 in. to 19.25 in. The geometric details for the specimens are given in Table B-2.

Specimen NRT-0R-3S400-4ST had a steel reinforcement ratio ( $2t_p/T$ ) of 2.25%. This is within the range (2-2.5%) of the US-APWR SRRC 2, and corresponds to US-APWR Section IDs 103 (south reactor cavity walls) and 104 (secondary shield walls) as shown in Table A-2.

Specimens NR-0R-3S400-4ST and NRC-0R-4S400-4ST had steel reinforcement ratios ( $2t_p/T$ ) of 3.60%. This is within the range (3-4%) of the US-APWR SRRC 4, and corresponds to US-APWR Section ID 105 (lower pressurizer walls) as shown in Table A-2.

Specimen NR-0R-3S200-4ST had a steel reinforcement ratio ( $2t_p/T$ ) of 4.50%. This is within the range (4-4.50%) of the US-APWR SRRC 5, and corresponds to US-APWR Section ID 106 (mid-height pressurizer walls) as shown in Table A-2..

All the specimens with names starting with B and S had steel reinforcement ratios ( $2t_p/T$ ) of 2.4%. The SRRC corresponding to these specimens is SRRC 2. The closest US-APWR sections are 102 (outer wall of RWSP with  $2t_p/T = 2.56\%$ ) and 103 (south reactor cavity wall with  $2t_p/T = 2.22\%$ ), as shown in Table A-2. Two of the specimens did not have any shear studs (B-4R-2S400-0ST and S-4R-2S400-0ST). The plate slenderness ratios ( $s/t_p$ ) for the specimens with shear studs, ranged from 22.2 to 44.4.

Specimen S-4R-0S-4ST did not have any shear reinforcement bars. Rest of the specimens had shear reinforcement; however, only one specimen had shear reinforcement spacing to depth ratio ( $s_{tie}/T$ ) that was within the limit to account shear reinforcement contribution in the design equations. The shear reinforcement spacing to depth ratio ( $s_{tie}/T$ ) was 0.5 for NR-0R-3S200-4ST and for the rest of the specimens this ratio ranged from 0.8 to 1.6. The US-APWR SC walls that correspond to the tested specimens have an  $s_{tie}/T$  ratio of at least 0.5. Therefore, the behavior and ductility of the US-APWR SC walls will be better than those of the specimens that did not have any shear reinforcement here. Nevertheless, the design criteria and strengths used in the design of SC walls in TeRs MUAP-11018 and MUAP-11019 are discussed with reference to the behavior of these tested specimens.

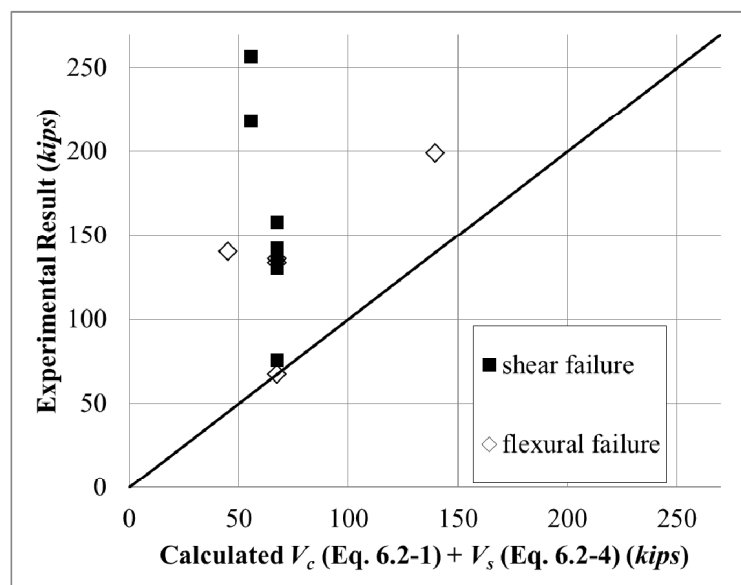


**Figure B-2 Experimental Results Comparisons with TeR MUAP-11019 Section 6.2 Shear Strength Equations (Eq 6.2-1 + Eq 6.2-4)**

Figure B-2 shows comparisons of the experimental results for the 13 specimens including those both with and without shear reinforcement and compared calculated using summation of Equations 6.2-1 and 6.2-4 of TeR MUAP-11019. The specimens are categorized based on their failure mode as being either flexural or shear failure. As seen in the figure, the design

strength calculated using TeR MUAP-11019 equations conservatively predicts the shear strengths for all the specimens. Only one specimen resulted in shear strength having same as the design equation; however this specimen failed in flexure before reaching its shear strength capacity.

Lastly, an experimental test program has been carried out at Purdue University, Bowen Laboratory particularly towards obtaining shear strength of unreinforced SC beams. The shear span to depth ( $a/d$ ) ratio was kept in between 2.5 and 3.5. A total of five SC simply supported beams were tested. The specimens had only shear studs anchored to concrete but not any shear reinforcement. The geometric details for the specimens are given in Table B-3.

The specimens were designed so that in each specimen only one parameter was changed and keeping the rest unchanged from the reference specimen (SP1-1), to clearly observe its influence in the response. The parameters varied in this test group included the stud spacing (SP1-2), plate reinforcement ratio (SP1-3), shear span-to-depth ratio (SP1-4) and specimen scale ratio or depth (SP1-5). The scaled specimens were tested under three-point bending and the large-scale specimens were tested in four-point bending load configuration.

Specimen SP1-3 had a steel reinforcement ratio ( $2t_p/T$ ) of 4.17%. This is within the range (4-4.5%) of the US-APWR SRRC 5, and corresponds to US-APWR Section IDs 106 (mid-height pressurizer walls) as shown in Table A-2. The plate slenderness ratio ( $s/t_p$ ) for this specimen was twice of the corresponding US-APWR section, which was 16.0.

Specimens SP1-1, SP1-2, SP1-4, and SP1-5 had a steel reinforcement ratio ( $2t_p/T$ ) of 2.78%. This is within the range (2.5-3%) of the US-APWR SRRC 3, and corresponds to US-APWR Section ID 101 (upper pressurizer wall) as shown in Table A-2. The plate slenderness ratios ( $s/t_p$ ) for these specimens ranged from 20 to 48. This plate slenderness is larger than the corresponding  $s/t_p$  ratio (12) for US-APWR SC wall design for Section ID 101 as shown in Table A-2. Additionally, these specimens do not have any tie bars or connectivity between the two opposite steel faceplates.

Figure B-3 shows comparisons of the experimental results for the five specimens without shear reinforcement and compares them to the concrete shear strength contribution ( $V_c$ ) calculated using Equations 6.2-1 of TeR MUAP-11019. The comparison indicates that the shear strength is conservatively estimated by the TeR MUAP-11019 design equation for all the specimens. The US-APWR SC walls have closely spaced rectangular tie bars. The behavior and ductility of the US-APWR SC walls will be better than those of the specimens that did not have any shear reinforcement. Nevertheless, the design strengths for out-of-plane shear can be estimated conservatively using TeR MUAP-11019 design equations.

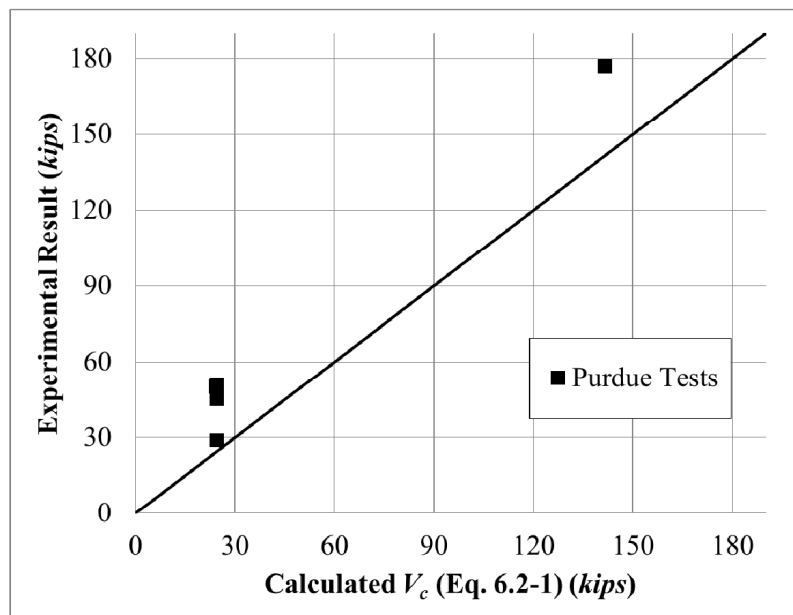


**Figure B-3 Experimental Results Comparisons with TeR MUAP-11019 Section 6.2  
Concrete Shear Strength Equations (Eq 6.2-1)**

## **Appendix C**

### **In-Plane Shear Database and Comparison with Design Equation**

## APPENDIX C

### TABLE OF CONTENTS

Appendix C. In-Plane Shear Database and Comparison with Design Equation .....	C-1
---	-----

### LIST OF FIGURES

Figure C-1 Experimental Results and Analytical Predictions for In-Plane Shear Specimens: (a) S200NN, (b) S300NN, (c) S400NN, and (d) Tri-linear Prediction Model Developed in TeR MUAP-11018 Appendix A. ....	C-3
Figure C-2 Comparison of Experimental In-Plane Shear Strength with Values Calculated using Equation 7.3-1 in TeR MUAP-11019. ....	C-4
Figure C-3 In-Plane Shear Force vs. Displacement Curves: (a) Effects of reinforcement ratio, (b) Effects of aspect ratio.....	C-7
Figure C-4 Comparison of Experimental In-Plane Shear Strength with Values Calculated Using ACI 349-06 and TeR MUAP-11019 Equations for In- Plane Shear Strength .....	C-8

### LIST OF TABLES

Table C-1 In-Plane Shear Tests of SC Wall Panels (References 12, 13) .....	C-2
Table C-2 In-Plane Shear Tests of SC Walls with Flanges (References 10, 11) .....	C-5

### **In-Plane Shear Database and Comparison with Design Equation**

This Appendix focuses on the experimental database of in-plane shear tests conducted on SC walls. The experimental database of SC wall in-plane shear tests is presented, and the test results are used to confirm the conservatism of the TeR MUAP-11019 Section 7.3 design equation for calculating the in-plane shear strength of SC walls.

The US-APWR SC walls are designed with more closely spaced shear studs and tie systems than all the specimens in the experimental database. Therefore, the test results provide conservative representations of the behavior and ductility of the US-APWR SC walls.

Table C-1 shows the experimental database of in-plane shear tests conducted on SC wall panels. Table C-1 includes experimental results from Kitano et al. 1997 (Reference 12) and Osuga et al. 2000 (Reference 13), which are listed in Table A-1. The specimens tested by Kitano et al. 1997 are most applicable to the US-APWR design and are discussed below.

Specimens S200NN, S215NN, and S230NN had steel reinforcement ratios ( $2t_p/T$ ) of 2.3%. This is within the range (2-2.5%) of the US-APWR SRRC 2, and corresponds to US-APWR Section IDs 103 (south reactor cavity walls) and 104 (secondary shield walls) as shown in Table A-2.

Specimens S200NN, S215NN, and S230NN are identical with the exception that they are subjected to zero axial force, compressive axial force equal to 353 kN, and compressive axial force equal to 706 kN, respectively. These axial compressive forces are small because they produce axial compressive stress ( $\sigma$ ) calculated as the compressive force divided by concrete area equal to 1.5 MPa and 3.0 MPa, respectively.

Similarly, specimens S300NN, S315NN, and S330NN had steel reinforcement ratios ( $2t_p/T$ ) of 3.2%. This is within the range (3 - 4%) of the US-APWR SRRC 4, and corresponds to US-APWR Section ID 105 (lower pressurizer walls) as shown in Table A-2. Specimens S300NN, S315NN, and S330NN were subjected to axial compressive forces equal to zero, 353 kN, and 706 kN, respectively.

Specimen S400NN had steel reinforcement ratio ( $2t_p/T$ ) of 4.5%, which is within the range (4-5%) of US-APWR SRRC 5, and corresponds to US-APWR Section ID 106 (mid-height pressurizer walls) as shown in Table A-2.

**Table C-1 In-Plane Shear Tests of SC Wall Panels (References 12, 13)**

--	--

Specimens S300PS and S300PN had center steel plates with and without studs, respectively. They are not included in this discussion because they do not have a direct correlation with the US-APWR SC wall design. Specimens S300HR and S300HN had circular penetrations with and without sleeves, respectively. They are not included in this discussion because they do not have direct correlations with the US-APWR SC wall design.

Seven specimens S200NN, S215NN, S230NN, S300NN, S315NN, S330NN, and S400NN are the focus of this discussion. They have plate slenderness ratio, defined as the shear stud spacing divided by plate thickness ( $s/t_p$ ), equal to 30. This plate slenderness is larger than the  $s/t_p$  ratios (8 – 16) for US-APWR SC wall design for all Section IDs as shown in Table A-2. Additionally, these specimens do not have any tie bars or connectivity between the two opposite steel faceplates. The US-APWR SC walls have closely spaced rectangular tie bars. Therefore, the behavior and ductility of the US-APWR SC walls will be better than those of the specimens discussed here. Nevertheless, the design criteria and strengths used in the design of SC walls in TeRs MUAP-11018 and MUAP-11019 are discussed with reference to the behavior of these tested specimens.

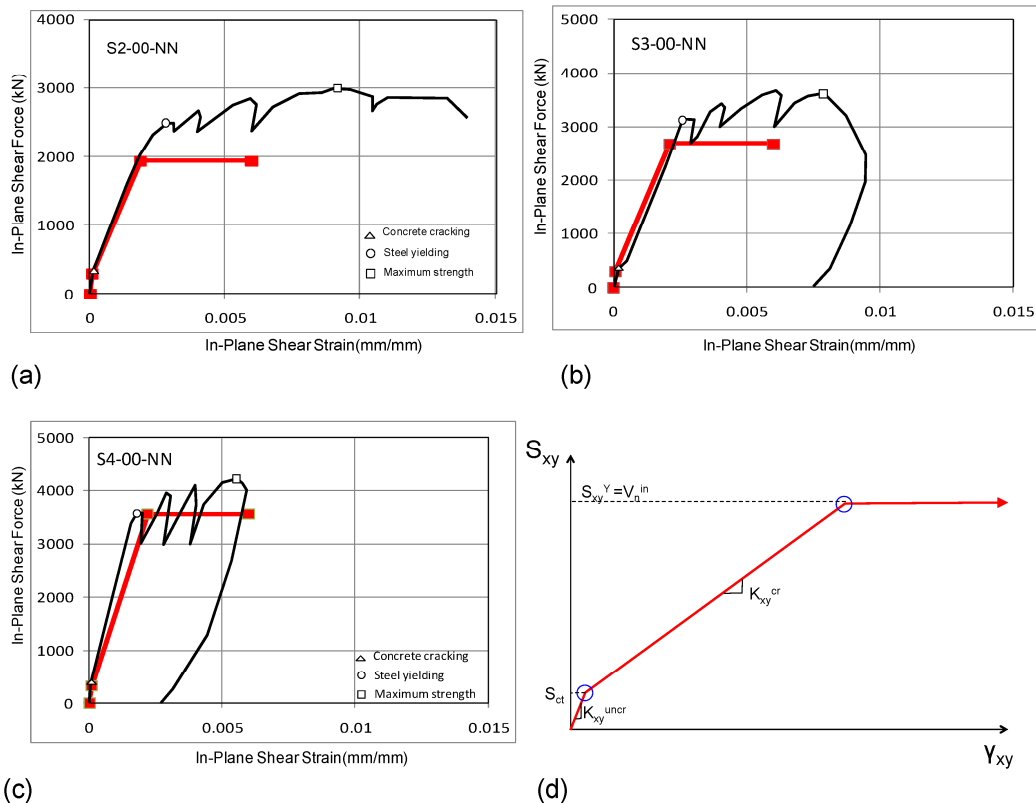


**Figure C-1 Experimental Results and Analytical Predictions for In-Plane Shear Specimens: (a) S200NN, (b) S300NN, (c) S400NN, and (d) Tri-linear Prediction Model Developed in TeR MUAP-11018 Appendix A.**

Specimens S200NN, S300NN, and S400NN were subjected to pure in-plane shear (with zero axial compression). The tests were conducted cyclically, and the envelopes of the measured cyclic in-plane shear force-shear strain ( $V$ - $\gamma$ ) responses are shown in Figure C-1. The figure also includes comparisons with the predicted tri-linear in-plane shear force-shear strain responses for the specimens, the details of which were presented in Appendix A of TeR MUAP-11018. These comparisons were also shown in Appendix B of TeR MUAP-11018.

Section 4 of TeR MUAP-11018 explains how the initial, tangent, and secant stiffness calculated using the tri-linear in-plane shear force-shear strain response are used to define the stiffness of the cracked and uncracked SC walls of US-APWR Containment Internal Structure. Additional, numerical comparisons of the predicted and measured initial and post-cracking stiffness of these specimens are included in Appendix B of TeR MUAP-11018.

Figure C-2 shows additional comparisons of the experimental results for the seven specimens (S200NN, etc. as listed above) with those calculated using Equation 7.3-1 in TeR MUAP-11019. The comparison focuses on the in-plane shear strength ( $S_{xy}^Y$ ) corresponding to Von Mises yielding of the steel faceplates. These comparisons were also included in Chapter 7 of TeR MUAP-11019. As shown, the TeR MUAP-11019 design equation conservatively predicts the in-plane shear strength of SC wall panels.

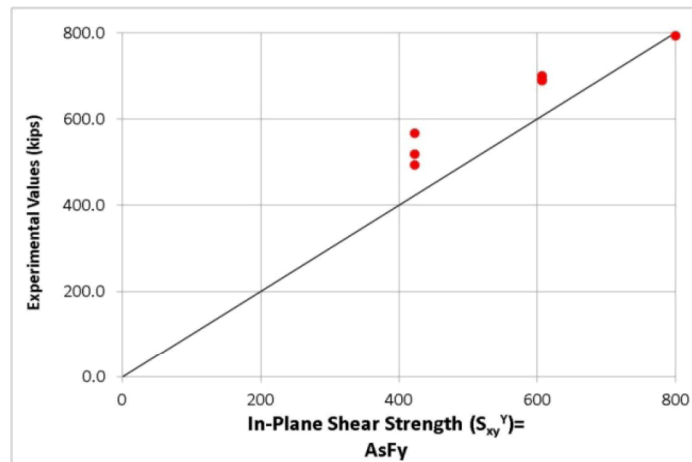


**Figure C-2 Comparison of Experimental In-Plane Shear Strength with Values Calculated using Equation 7.3-1 in TeR MUAP-11019.**

**Table C-2 In-Plane Shear Tests of SC Walls with Flanges (References 10, 11)**

--	--

Table C-2 presents the experimental database of in-plane shear (or lateral load) tests conducted on SC walls with flanges. Table C-2 includes experimental results from Funakoshi et al. 1998 (Reference 10) and Fujita et al. 1998 (Reference 11), which are listed in Table A-1. The discussion below focuses on the specimens tested by Funakoshi et al. 1998 (Reference 10).

The specimens tested by Fujita et al. (Reference 11) are not included in this discussion because those tests focused on the lateral load behavior of SC walls connected to the concrete basemat using anchor rods. Those tests focused on an SC wall-to-basemat connection, which is very different from the US-APWR SC wall-to-basemat connection.

As shown in Table C-2, the two main test parameters were steel ratio ( $T/t_p$  = the wall thickness to the steel plate thickness) and shear span ratio ( $H/L$ ). The term  $H$  represents the effective wall height (the distance from the top surface of the concrete block to the center line of the loading) and the term  $L$  represents the length of the specimen in the direction of the lateral loading applied.

Specimen BS70T05 had steel ratio ( $T/t_p$ ) of 51, which corresponds to steel reinforcement ratio ( $2t_p/T$ ) of 3.91%. It is within the range (3.0-4.0%) of the US-APWR SRRC 4 and the corresponding US-APWR Section ID is 105 (lower pressurizer walls). Specimens BS50T10, BS70T10, and BS85T10 had steel ratios ( $T/t_p$ ) of 100 and they are equivalent of steel reinforcement ratios ( $2t_p/T$ ) of 2.0%. Specimen BS70T14 had steel ratio ( $T/t_p$ ) of 144 and its steel reinforcement ratio ( $2t_p/T$ ) of 1.39%. The US-APWR SRRC for these specimens is SSRC-1, and corresponds to US-APWR Section ID 107 (refueling and reactor cavity walls) and 108 (north refueling cavity walls).

Specimen BS50T10 had shear span ratio ( $H/L$ ) of 0.5 and specimen BS85T10 had shear span ratio of 0.85. Specimens BS70T05, BS70T10, and BS70T14 had shear span ratios ( $H/L$ ) of 0.7. Specimens BS70T05, BS50T10, BS70T10, BS85T10, and BS70T14 were subjected to in-plane shear (with zero axial compression). The tests were conducted cyclically, and the envelopes of the measured cyclic in-plane shear force-displacement responses are shown in Figure C-3. The figure includes the effects of steel reinforcement ratio ( $t_p/T$ ) and shear span ratio ( $H/L$ ) on the in-plane shear – displacement responses.

The experimental results indicate that the initial stiffness and cracking points for shear deformation increased slightly with increase of the steel web plate thickness,  $t_p$ . However, no pronounced difference was observed since the behavior is dominated by the concrete infill. The shear yield load and maximum load increased significantly with increases in the web steel plate thickness,  $t_p$ . In addition, the stiffness decreased significantly as  $H/L$  ratio increased. The maximum load appears to be larger as  $H/L$  decreased.

Figure C-4 shows additional comparisons of the experimental results for the five test specimens with in-plane shear strength predicted by ACI 349-06 and TeR MUAP-11019 in-plane shear strength equations. The experimentally measured ultimate in-plane shear strength was divided by in-plane shear strength predicted using both equations. The ACI 349-06 equation for in-plane shear strength of reinforced concrete walls is shown in Equation C-1.

$$\text{Equation C-1} \quad V_N = A_s f_y + \alpha_c \left( 1 + \frac{N_u}{2000 A_g} \right) \sqrt{f'_c} A_c$$

Where,

- $N_u$  is axial force normal to cross-section and  $A_g$  is gross area of concrete section.
- For the application to flanged SC walls, flange area that intersects the web is also taken account in addition to gross area of web portion of flanged SC walls.
- $b_w$  is web width and  $d$  is distance from extreme compression fiber to centroid of longitudinal tension reinforcement.
- $\alpha_c$  is the coefficient that is equal to 3.0 for wall aspect (H/L) ratio less than 1.5, and 2.0 for H/L greater than 2.0, and varies linearly between 3.0 and 2.0 for H/L ratios between 1.5 and 2.0.
- $A_s$  is the area of the steel plates ( $A_s = A_{cv}\rho_t$ ) of the web in addition to the steel plate area in flange that intersects the web.
- $f_y$  is the specified yield strength for the steel plates

The TeR MUAP-11019 Section 6.3 equation is the similar to Equation C- with the exception that the concrete contribution to the in-plane shear strength is ignored as shown in Equation C-.

**Equation C-2**

$$V_N = A_s f_y$$

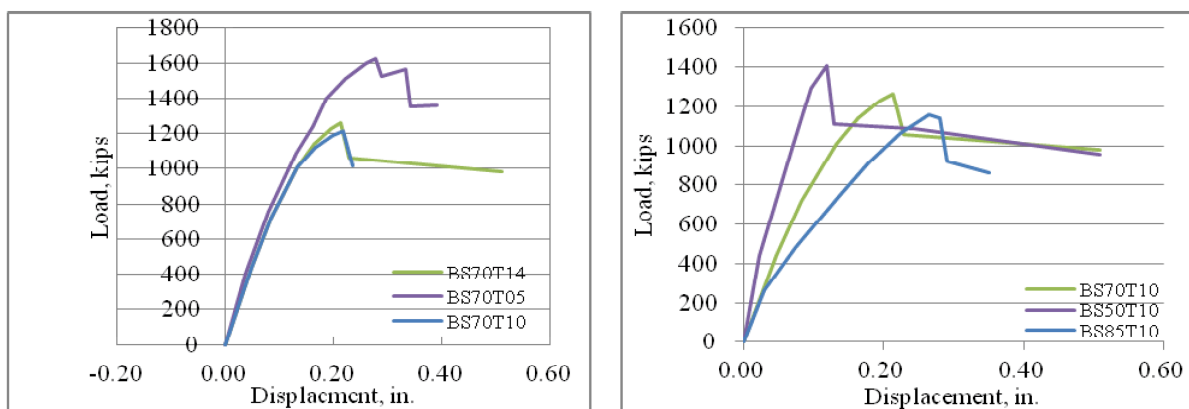


**Figure C-3 In-Plane Shear Force vs. Displacement Curves: (a) Effects of reinforcement ratio, (b) Effects of aspect ratio**

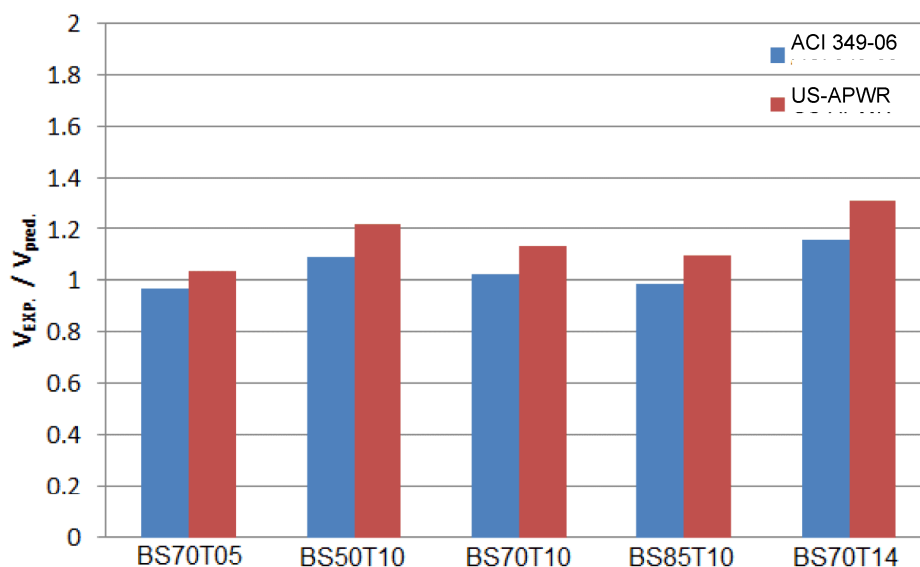


**Figure C-4 Comparison of Experimental In-Plane Shear Strength with Values Calculated Using ACI 349-06 and TeR MUAP-11019 Equations for In-Plane Shear Strength**

As shown in Figure C-4, the TeR MUAP-11019 design equation conservatively predicts the in-plane shear strength of SC wall specimens with flanges irrespective of the steel reinforcement ratio or the wall aspect ratio (H/L).

## **Appendix D**

### **Axial Compression and Local Buckling Database and Comparison with Design Equation**

## APPENDIX D

### TABLE OF CONTENTS

Appendix D Axial Compression and Local Buckling Database and Comparison with Design Equation .....	D-1
---	-----

### LIST OF FIGURES

Figure D-1 Axial Load-Displacement Curves from Tests by Kanchi et al. (1996) (Reference 15). ....	D-2
Figure D-2 Local Buckling vs. Slenderness Ratio Experimental Database .....	D-4
Figure D-3 Test Setup for Thermal Tests by Sekimoto et al. (2001) (Reference 8).....	D-7
Figure D-4 Test Results from Thermal Tests by Sekimoto et al. (2001) (Reference 8) .....	D-8

### LIST OF TABLES

Table D-1 Compression Loading Tests (References 14, 15, 16) .....	D-3
Table D-2 Thermal Behavior Tests (References 8, 9).....	D-6

### **Axial Compression and Local Buckling Database and Comparison with Design Equation**

This Appendix focuses on the experimental database of axial compression tests conducted on SC walls and the local buckling behavior of steel faceplates. The experimental database of SC wall compression tests is presented, and the test results are used to confirm the conservatism of the TeR MUAP-11019 recommended maximum plate slenderness ratio of 20.

Table D-1 presents the database of compression tests conducted on SC wall stub columns. It includes experimental results from Usami et al. (1995), Kanchi et al. (1996) and Sekimoto et al. (1996) (References 14, 15 and 16, respectively).

The main parameter in Table D-1 is the plate slenderness ratio ( $s/t_p$ ), which is calculated as the largest clear spacing ( $s$ ) of the steel headed stud anchors, structural shapes, or tie bars divided by the steel faceplate thickness ( $t_p$ ). The specimens dimensions, loading setups, and test results are also included in the database).

As shown in Table D-1, Usami et al. (1995) (Reference 14) conducted four cyclic compression tests. Specimens NS20, NS30, NS40 and NS50 had steel reinforcement ratios ( $2t_p/T$ ) of 3.24%, which is within the range (3%-4%) of the US-APWR SRRC 4, and corresponds to US-APWR Section ID 105 (lower pressurizer walls). However, the steel reinforcement ratio ( $2t_p/T$ ) is not a relevant parameter for the compression tests. The steel plate slenderness is the primary parameter of interest because it governs the local buckling of the steel faceplates and thus the axial compression strength.

Specimens N20, N30, N40 and N50 had plate slenderness ratios ( $s/t_p$ ) of 20, 30, 40 and 50, respectively. These  $s/t_p$  ratios are much larger than the  $s/t_p$  ratios (8-16) for US-APWR SC wall design for all section IDs as shown in Table A-2. TeR MUAP-11019 Section 2.2 recommends that the plate slenderness ratio ( $s/t_p$ ) limit is 20. Local buckling of the steel faceplates will occur before yielding for SC walls and specimens with  $s/t_p$  ratio greater than 20. This is confirmed by the test results for all the specimens.

As shown in Table D-1, Kanchi et al. (1996) (Reference 15) conducted 11 compression tests. The compressive load was uni-directional but cyclic (load-unload-reload cyclic). The SC walls had  $s/t_p$  ratios that are greater than the  $s/t_p$  ratios (8-16) for US-APWR SC wall design for all section IDs. The failure was typically due to local buckling of the steel faceplates. .

Specimens C4-20M, C4-25M, C4-30M, C4-50M and C4-30S had steel reinforcement ratios ( $2t_p/T$ ) of 3.21%. This is within the range (3%-4%) of the US-APWR SRRC 4, and corresponds to US-APWR Section ID 105 (lower pressurizer walls). However, the steel reinforcement ratio ( $2t_p/T$ ) is not a relevant parameter for the compression tests. The steel plate slenderness is the primary parameter of interest because it governs the local buckling of the steel faceplates and thus the axial compression strength. Specimens C4-20M, C4-25M, C4-30M, C4-50M had 0.18 inch (4.5 mm) faceplates with plate slenderness ratios ( $s/t_p$ ) of 20, 25, 30 and 50, respectively. C4-30S had 0.18 inch (4.5 mm) faceplates with  $s/t_p$  ratio of 30, but the yield stress of the steel was lower than C4-30M.

Specimens C6-20M, C6-25M, C6-30M, C6-35M, C6-40M and C6-30S had steel reinforcement ratios ( $2t_p/T$ ) of 4.29%. This is within the range (4%-5%) of the US-APWR SRRC 5, and corresponding to US-APWR Section ID 106 (mid-height pressurizer walls). However, the steel reinforcement ratio ( $2t_p/T$ ) is not a relevant parameter in compression tests. The steel plate

slenderness is the primary parameter of interest because it governs the local buckling of the steel faceplates and thus the axial compression strength. Specimens C6-20M, C6-25M, C6-30M, C6-35M, C6-40M and C6-30S had 0.24 in. (6 mm) thick steel faceplates with  $s/t_p$  ratios of 20, 25, 30, 35 and 40, respectively. C6-30S had 0.24 in. (6 mm) faceplates with  $s/t_p$  ratio of 30, but the yield stress of the steel was lower than C6-30M.

Figure D-1 (a) and (b) show the axial load-displacement curves for C4 test series and C6 test series, respectively. The results indicate that the compressive strength of the SC walls decrease with increase of the  $s/t_p$  ratio. In addition, the local buckling occurred before yielding of the steel faceplates for specimens with  $s/t_p$  ratios from 25 to 50. This is not applicable to the US-APWR SC design with  $s/t_p$  ratios of 8-16, where faceplate yielding will occur prior to local buckling.

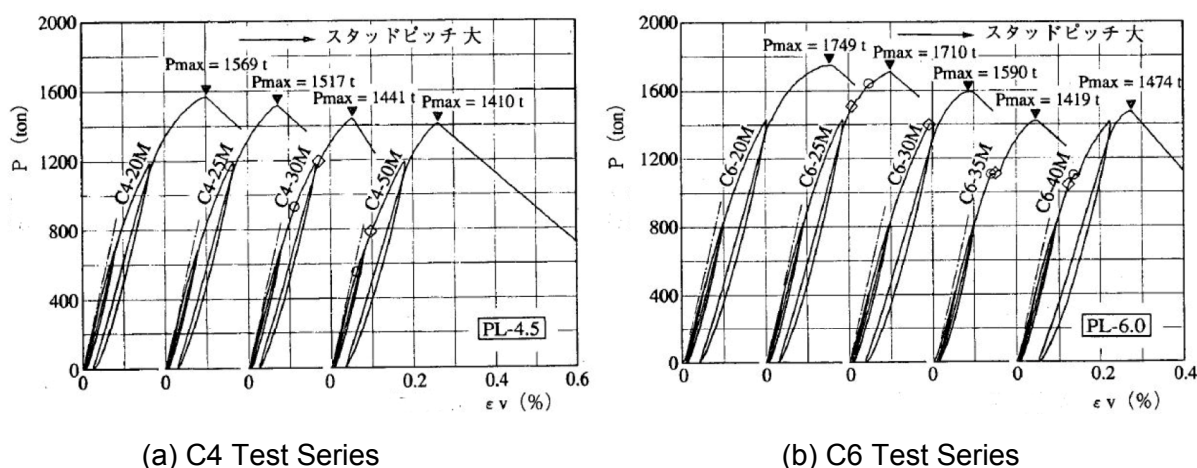


**Figure D-1 Axial Load-Displacement Curves from Tests by Kanchi et al. (1996)  
(Reference 15).**

As shown in Table D-1, Sekimoto et al. (1996) (Reference 16) conducted three cyclic compression tests. Specimens NS50, NS75 and NS100 had steel reinforcement ratios ( $2t_p/T$ ) of 2.60%. This is within the range (2%-3%) of the US-APWR SRRC 3, and corresponds to US-APWR Section ID 109. However, the steel reinforcement ratio ( $2t_p/T$ ) is not a relevant parameter in compression tests. The steel plate slenderness is the primary parameter of interest because it governs the local buckling of the steel faceplates and thus the axial compression strength. Specimens N50, N75, and N100 had plate slenderness ratio ( $s/t_p$ ) of 50, 75, and 100, respectively. These  $s/t_p$  ratios are much larger than the  $s/t_p$  ratios (8-16) for US-APWR SC wall design for all section IDs. The failure was due to local buckling of the steel faceplates.

**Table D-1 Compression Loading Tests (References 14, 15, 16)**

--	--

The experimental results from all the tests in the experimental database have been compiled and plotted in Figure D-2. The ordinate in the plot is the normalized strain,  $\varepsilon_{cr}/\varepsilon_y$ , where  $\varepsilon_{cr}$  is the critical buckling strain of the steel plate from compressive tests and  $\varepsilon_y$  is the nominal yield strain of the steel plates. The abscissa is the plate slenderness ratio ( $s/t_p$ ) normalized with respect to the square root of  $E/F_y$ , where  $E$  is the Young's modulus of steel. Euler's column buckling curve with effective length coefficient ( $K$ ) equal to 0.7 is also plotted in the figure. It can be observed that the test data points have a trend that follows Euler's curve.

Another important observation is that there is no data that falls in the shadowed area where the normalized slenderness ratio is less than 1.0 and  $\varepsilon_{cr}$  is less than  $\varepsilon_y$ . This implies that when the normalized plate slenderness  $[s/t_p \times \sqrt{F_y/E}]$  ratio is less than 1.0, yielding ( $\varepsilon_y$ ) occurs before local buckling ( $\varepsilon_{cr}$ ). This leads to the conclusion that the slenderness ratio limit for non-compactness, i.e., yielding before local buckling in compression is given by Equation D-1.

$$\text{Equation D-1} \quad \frac{s}{t_p} \leq 1.0 \sqrt{\frac{E}{F_y}}$$

For steel faceplates with yield stress ( $F_y$ ) equal to 50 ksi, Equation D-1 results in  $s/t_p$  ratio limit of 24. However, TeR MUAP-11019, Section 2.2 provides a more conservative limit of 20 for the US-APWR SC walls. Additionally, as shown in Table A-2, all the US-APWR SC walls have  $s/t_p$  ratios within the range of 8-16, much lower than the limit.

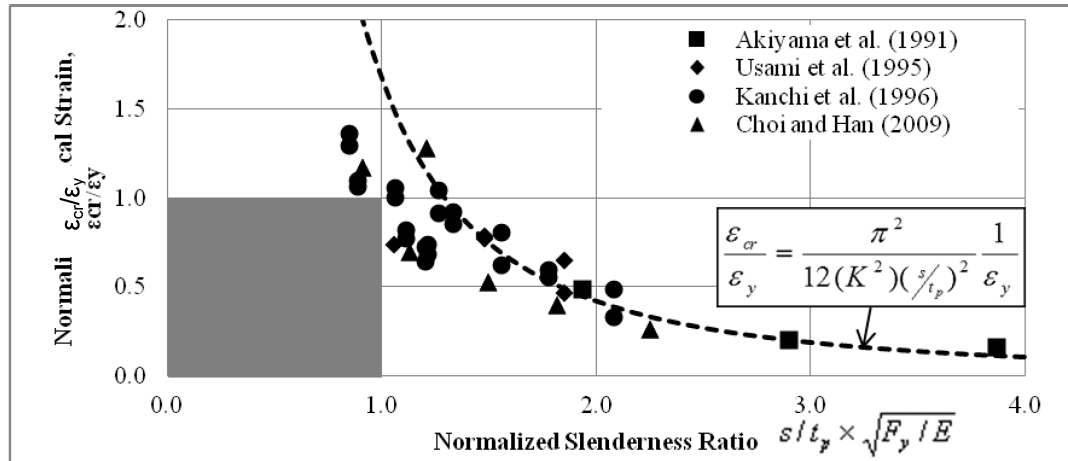


Figure D-2 Local Buckling vs. Slenderness Ratio Experimental Database

Table D-2 includes experimental results from Sekimoto et al. (2001) and Sekimoto et al. (2003) (References 8 and 9, respectively, as listed in Table A-1 of the experimental database). The main parameter is the plate slenderness ratio ( $s/t_p$ ). SC walls were tested to investigate the effects of thermal loading on concrete cracking and the local buckling of the steel faceplates if the thermal deformation is restrained. The  $s/t_p$  ratios ranged from 10 to 45. Local buckling of the steel faceplates occurred only for the specimen with the significant large  $s/t_p$  ratio of 45. The temperature was increased up to 300 °C (572 °F) and most of the specimens only had cracking due to thermal gradient. The specimens' dimensions, loading setups, and test results are included in the database and in Figure D-3 and Figure D-4.

Specimens reported in Sekimoto et al. (2001) and Sekimoto et al. (2003), as shown in Table D-2, had steel reinforcement ratios ( $2t_p/T$ ) of 1.13% and 1.17%, respectively. This is within the range (1%-2%) of the US-APWR SRRC 2, and corresponds to US-APWR Section ID 103 (south reactor cavity walls). The local buckling behavior of SC wall faceplates is governed by  $s/t_p$  ratio, and the steel reinforcement ratio is not a relevant parameter for evaluating the local buckling of the steel faceplates. The US-APWR SC walls have  $s/t_p$  ratios less than 16, which are not susceptible to local buckling before yielding.

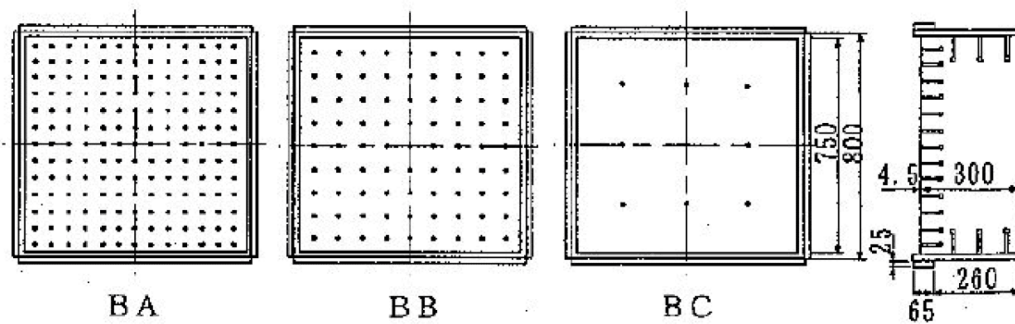
Specimens BA, BB and BC reported by Sekimoto et al. (2001) (Reference 8) had  $s/t_p$  ratios of 12.4, 17.8 and 45.3, respectively. As shown in Figure D-3, the steel faceplates of the specimens were subjected to heating (thermal loading), and their ends were fully restrained to prevent any expansion. The steel faceplates were subjected to axial compressive stress associated with  $(-\alpha_s \Delta T E)$  the restrained thermal strain.

As shown in Figure D-4, for Specimens BA and BB, local buckling could not be observed visually even when the temperature was increased to 300 °C (572 °F). Faceplate local buckling occurred only for Specimen BC with plate slenderness ratio ( $s/t_p$ ) ratio of 45.3. For this specimen, heating was terminated after Step 3 (100 °C, 212 °F). Neither fracture nor pull out of shear studs occurred.

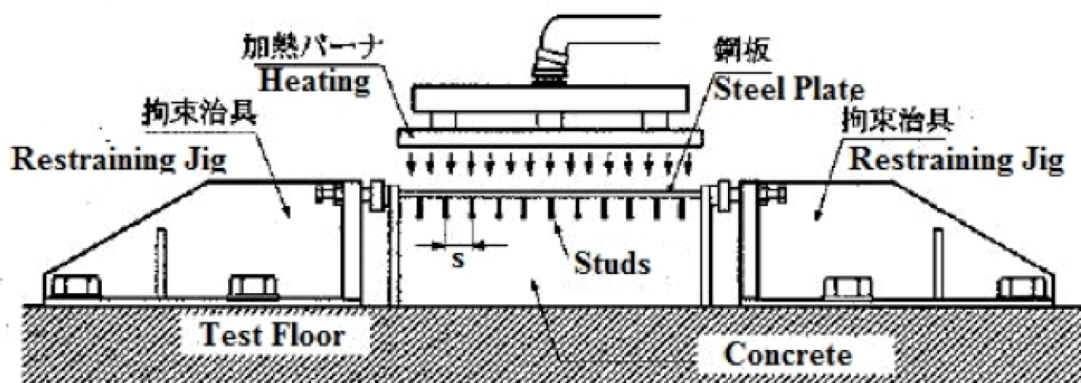
The tests described above confirm that the US-APWR maximum plate slenderness ratio of 20 described in TeR MUAP-11019 Section 2.2 is conservative in preventing steel plate local buckling

**Table D-2 Thermal Behavior Tests (References 8, 9)**

--	--



(a) Specimen Dimensions



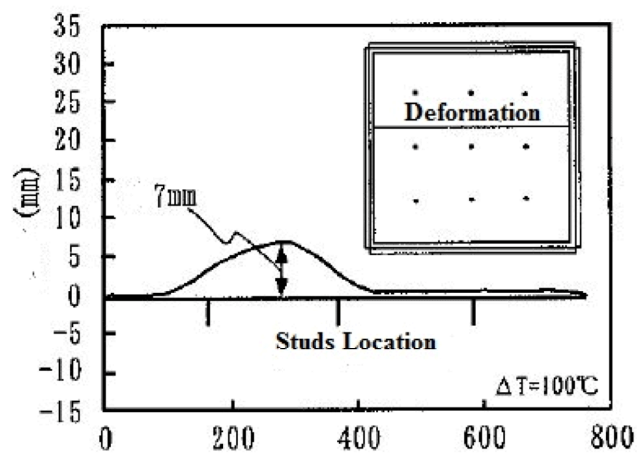
(b) Overview of Test Setup

(b) Overview of Test Setup

Figure D-3 Test Setup for Thermal Tests by Sekimoto et al. (2001) (Reference 8)

Step	Temperature, Degree C	BA	BB	BC
1	50	None	None	None
2	75	None	None	None
3	100	None	None	Buckling
4	150	None	None	
5	200	None	None	
6	250	None	None	
7	300	None	None	

(a) Occurrence of Steel Faceplate Buckling



(b) Deformation of Steel Faceplate (Specimen BC)

**Figure D-4 Test Results from Thermal Tests by Sekimoto et al. (2001) (Reference 8)**

## Appendix E – Research References

1. Takeuchi, M; et al; “Experimental Study on Steel Plate Reinforced Concrete Structure Part 28 Response of SC Members Subjected to Out-of-plane Load (Outline of the Experimental Program and the Results)”, Annual Meeting Architectural Institute of Japan., 1999, pp. 1237-1238
2. Hong, S; et al; (2009) “Out-of-Plane Shear Strength of Steel Plate Reinforced Concrete Walls Dependent on Bond Behavior”, Journal of Disaster Research Vol.5 No.4, 2010
3. Varma, A.H.; Sener, K.C.; Zhang, K.; Coogler, K; and Malushte, S.R.; (2011). “Out-of-Plane Shear Behavior of SC Composite Structures.” Trans. of the Internal Assoc. for Struct. Mech. in Reactor Tech. Conf., SMiRT-21, Div-VI: Paper ID# 763, 6-11, New Delhi, India, November, 2011
4. Akiyama, H; et al; “1/10 th Scale Model Test of Inner Concrete Structure Composed of Concrete Filled Steel Bearing Wall”, SMiRT-10, 1989
5. Akita, S; et al; “A Study on the Structural Performance of SC Thick Walls Part 1 Experiment of the SC Thick Wall, Part 2 and Part 3 Pretest Analysis of the SC Thick Walls”, Annual Conference of Architectural Institute of Japan, 2003, pp. 1027- 1032)
6. Akita, S; et al; “Experiment for Fire Resistance of A Concrete Filled Steel Structure Part 1 and Part 2. Bearing Wall (Outline of experimental program and the results)”, Annual Conference of Architectural Institute of Japan, 1997, pp. 171-174
7. Kanchi, M; et al; “Experiment for Fire Resistance of a Concrete Filled Steel Structure Part 6 and Part 7 Bearing Wall”, Annual Conference of Architectural Institute of Japan, 1999, pp. 71-74
8. Sekimoto, H; et al; “Study on Property of Concrete-filled Steel-bearing Wall Subjected to High Temperature”, Journal of Structural Engineering. B, VOL.47B, pp481-490, 2001
9. Sekimoto, H; et al; “Experimental Study on Property of SC Structure Subjected to High Temperature Hysteresis”, Journal of Structural Engineering. B, VOL.49B, pp391-399, 2003
10. Funakoshi, A.; Akita, S.; Matsumoto, H.; Hara, K., Matsuo, I.; and Hayashi, N. “Experimental Study on A Concrete Filled Steel Structure Part. 7 thru Part 9 Bending Shear Tests”, Annual Meeting of Architectural Institute of Japan, 1998, pp. 1063-1068

11. Fujita, T.; Funakoshi, A.; Akita, S.; Matsuo, I.; et al; "Experimental Study on A Concrete Filled Steel Structure Part. 14 thru Part 17 Bending Shear Tests", Summaries of Technical Papers of Annual Meeting, Architectural Institute of Japan, 1998, pp. 1121-1128
12. Kitano, T.; Akita, S., Nakazawa, M.; Fujino, Y.; Ohta, H.; Yamaguchi, T.; Nakayama, T.; "Experimental Study on a Concrete-filled Steel Structure Part 4: Shear Tests (Outline of the experimental program and the results)", Summaries of Technical Papers of Annual Meeting, Architectural Institute of Japan. B-2, pp. 1057-1058, 1997
13. Masahiko, O.; Shodo, A.; Masayuki, T.; Hirosuke, O.; Tatsuo, N.; Hironori, N.; "Experimental Study on Steel-plate-reinforced Concrete Structure Part. 41-43 Heating Tests", Summaries of Technical Papers of Annual Meeting, Architectural Institute of Japan, 2000, pp. 1127-1132
14. Usami, S.; Akiyama, H., Narikawa, M.; Hara, K.; Takeuchi, M.; and Sasaki, N.; "Study on a concrete filled steel structure for nuclear power plants (part 2). Compressive loading tests on wall members", SMiRT-13, Porto Alegre, Brazil, August, 1995
15. Kanchi, M.; et al, "Experimental Study on Concrete-filled Steel Structure: Part 2 Compressive Tests Characteristics Test (1)", Summaries of technical papers of Annual Meeting Architectural Institute of Japan. B-2, Structures II, Structural dynamics nuclear power plants 1996, 1071-1072, 1996-07-30
16. Sekimoto, H., "Experimental Study on Concrete Filled Steel Shear Wall: Part 1 Compression Test of Seismic Wall", Summaries of technical papers of Annual Meeting Architectural Institute of Japan. Structures II 1991, 1659-1660, 1991-08-01
17. Akita, S; Ozaki, M; "Earthquake-Resistant Design Recommendation for Building Using Steel Plate Reinforced Concrete Structure (Design Method of Earthquake-Resistant Wall)", Technical Report of Architectural Institute of Japan, Dec., 2001, No.14, pp123-128
18. Ozaki, M. et al, "Study on Steel Plate Reinforced Concrete Panels Subjected to Cyclic In-Plane Shear", Nuclear Engineering and Design, Volume 228, 2004
19. Varma, A.; Malushte, S.; Sener, K.; Both, P.; Coogler, K.; "Steel-Plate Composite (SC) Walls: Analysis and Design Including Thermal Effects", SMiRT 21, New Delhi, India, November 2011

## **Reference 1**

### **Experimental Study on Steel Plate Reinforced Concrete Structure Part 28 Response of SC Members Subjected to Out-of-Plane Load**

















## **Reference 2**

### **Out-of-Plane Shear Strength of Steel-Plate-Reinforced Concrete Walls Dependent on Bond Behavior**



















## **Reference 3**

### **Out-Of-Plane Shear Behavior of SC Composite Structures**

















## **Reference 4**

### **1/10th Scale Model Test of Inner Concrete Structure Composed of Concrete Filled Steel Bearing Wall**













## **Reference 5**

### **A Study on the Structural Performance of SC Thick Walls**











































## **Reference 6**

### **Experiment for Fire Resistance of A Concrete Filled Steel Structure**























## **Reference 7**

### **Experiment for Fire Resistance of a Concrete Filled Steel Structure**

























## **Reference 8**

### **Study on Property of Concrete-filled Steel-bearing Wall Subjected to High Temperature**



































































## **Reference 9**

### **Experimental Study on Property of SC Structure Subjected to High Temperature Hysteresis**





















































## **Reference 10**

### **Experimental Study on A Concrete Filled Steel Structure**







































































## **Reference 11**

### **Experimental Study on A Concrete Filled Structure**



























## **Reference 12**

### **Experimental Study on a Concrete-filled Steel Structure**















## **Reference 13**

### **Experimental Study on Steel-plate-reinforced Concrete Structure**









































## **Reference 14**

**Study on a concrete filled steel structure for  
nuclear power plants (part 2). Compressive  
loading tests on wall members**













## **Reference 15**

### **Experimental Study on Concrete-filled Steel Structures**

















## **Reference 16**

### **Experimental Study on Concrete-filled Steel Shear Wall**



















## **Reference 17**

**Earthquake-Resistant Design Recommendation  
for Building Using Steel Plate Reinforced  
Concrete Structure (Design method for  
earthquake-resistant wall)**

























































## **Reference 18**

### **Study on Steel Plate Reinforced Concrete Panels Subjected to Cyclic In-plane Shear**









































## **Reference 19**

### **Steel-Plate Composite (SC) Walls: Analysis and Design Including Thermal Effects**















